AGU PUBLICATIONS

Water Resources Research

RESEARCH ARTICLE
10.1002/2014WR016841

Special Section:
The 50th Anniversary of Water Resources Research

Geomechanics of subsurface water withdrawal and injection

Giuseppe Gambolati[1] and Pietro Teatini[1]

[1]Department of Civil, Architectural and Environmental Engineering, University of Padova, Padova, Italy

Abstract Land subsidence and uplift, ground ruptures, and induced seismicity are the principal geomechanic effects of groundwater withdrawal and injection. The major environmental consequence of groundwater pumping is anthropogenic land subsidence. The first observation concerning land settlement linked to subsurface processes was made in 1926 by the American geologists Pratt and Johnson, who wrote that "the cause of subsidence is to be found in the extensive extraction of fluid from beneath the affected area." Since then, impressive progress has been made in terms of: (a) recognizing the basic hydrologic and geomechanic principles underlying the occurrence; (b) measuring aquifer compaction and ground displacements, both vertical and horizontal; (c) modeling and predicting the past and future event; and (d) mitigating environmental impact through aquifer recharge and/or surface water injection. The first milestone in the theory of pumped aquifer consolidation was reached in 1923 by Terzaghi, who introduced the principle of "effective intergranular stress." In the early 1970s, the emerging computer technology facilitated development of the first mathematical model of the subsidence of Venice, made by Gambolati and Freeze. Since then, the comprehension, measuring, and simulation of the occurrence have improved dramatically. More challenging today are the issues of ground ruptures and induced/triggered seismicity, which call for a shift from the classical continuum approach to discontinuous mechanics. Although well known for decades, anthropogenic land subsidence is still threatening large urban centers and deltaic areas worldwide, such as Bangkok, Jakarta, and Mexico City, at rates in the order of 10 cm/yr.

Key Points:
- Major geomechanical effects of groundwater withdrawal and water injection
- Numerical modeling of geomechanics as related to water withdrawal and injection
- Advances in measuring ground displacement by satellite technology

Correspondence to:
G. Gambolati,
gambo@dmsa.unipd.it

Citation:
Gambolati, G., and P. Teatini (2015), Geomechanics of subsurface water withdrawal and injection, *Water Resour. Res.*, *51*, 3922–3955, doi:10.1002/2014WR016841.

Received 30 DEC 2014
Accepted 4 MAY 2015
Accepted article online 13 MAY 2015
Published online 7 JUN 2015

1. Introduction

Geomechanics is the branch of science concerned with the equilibrium and movement of rock deposits [*Verruijt*, 1995], where rock is to be understood as the natural material in the upper portion (say between 100 and 1000 m depth) of the earth's crust. At variance with geotechnique, which focuses mainly on the interaction between soil and man-made structures and thus investigates shallow-depth local-scale processes, geomechanics addresses regional (or basin-scale) environmental issues involving the development and use of subsurface water resources.

Groundwater geomechanics is concerned with the ground deformation processes induced by subsurface water pumping and injection. A number of geomechanical factors at both the withdrawn/injected formation and the ground surface level are worth considering in groundwater geomechanics. These include:

1. Lowering of the ground surface, i.e., land subsidence, as a consequence of aquifer overdraft worldwide [e.g., *Gambolati et al.*, 1991; *Ortega-Guerrero et al.*, 1999; *Holzer and Galloway*, 2005; *Teatini et al.*, 2006; *Shi et al.*, 2007; *Allis et al.*, 2009; *Mahmoudpour et al.*, 2013];
2. Upheaval of the ground surface due to the injection of water (or water-based fluids) into subsurface formations [e.g., *Bawden et al.*, 2001; *Bell et al.*, 2008; *Teatini et al.*, 2011b];
3. The formation of earth fissures caused by groundwater pumping in subsiding basins. The movement of blocks adjacent to a fissure is usually perpendicular to the plane identified by the fissure [e.g., *Holzer and Pampeyan*, 1981; *Bankher and Al-Harthia*, 1999; *Wang et al.*, 2009; *Carreón-Freyre et al.*, 2010];
4. The activation of preexisting shallow faults, creating a failure of the land surface. The failure is usually associated with a significant component of the relative displacement of blocks parallel to the faulting plane [e.g., *Li et al.*, 2000; *Carreón-Freyre et al.*, 2011; *Huizar-Álvarez et al.*, 2011];
5. Inducing or triggering microseismic and seismic events because of changes in of the natural effective and total stress regimes [e.g., *Frohlich*, 2012; *González et al.*, 2012; *Horton*, 2012; *Ellsworth*, 2013; *Holland*, 2013].

Almost one century has passed since scientists started to investigate these occurrences to any considerable extent. In the sequel land subsidence, the most widespread and studied geomechanical response to groundwater pumping is first addressed. A historical review is followed by a discussion of the main factors controlling the process and the basic principles and equations underlying it, in light of continuous progress in mathematical and numerical modeling. The opposite occurrence, i.e., the upheaval of land surface induced by artificial water injection into the subsurface, is also reviewed. Although important advances have been made in simulating continuous land displacements (i.e., land subsidence and uplift), a few processes are still poorly understood, such as the influence of differential vertical compaction, horizontal displacements, and discontinuity in the bedrock on near-surface ground ruptures, fissure generation, and fault reactivation. Induced seismicity associated with overexploitation or overpressurization of subsurface formation must also be investigated in depth. The most advanced tools for recording and monitoring ground deformation and surface displacements are mentioned. Finally, the discussion focuses on the connection between research into groundwater geomechanics and the present challenges to be met in undertaking effective remedial measures aimed at mitigating the associated environmental and socioeconomic impacts.

2. Historical Retrospective

The first observation relating land subsidence to subsurface fluid removal was made in 1926 by the American geologists *Pratt and Johnson* [1926], who discussed the origin of the settlement noticed in the Gaillard peninsula, the center of Goose Creek Oil Field, Galveston Bay (TX), and concluded that "the Goose Creek subsidence was directly caused by the extraction of oil, water, gas, and sand from beneath the surface beginning in the year 1917." They also made a conjecture concerning the mechanism governing the underlying process, postulating that "the pore spaces are occupied by water draining more slowly from the adjacent clays; and it is a well-known fact that the draining of clays causes them to become more compact, and this in turn would permit subsidence of overlying surface." However, a few years earlier, *Fuller* [1908] had already theorized that fluid withdrawal and a decrease in fluid pore pressure caused the sinking of the land surface because of the removal of hydrostatic support. *Pratt* [1927] and *Snider* [1927] raised some questions concerning the actual cause of the subsistence and attempted to provide answers.

It is interesting to note how the general public's perception of anthropogenic land subsidence has drastically changed over time. Today, the occurrence of settlement affecting large areas is a matter of great concern from a variety of viewpoints involving economic, environmental, and safety issues. No one would gladly be recognized as responsible for generating land subsidence, and in regions where ground sinking is caused by both groundwater pumping and hydrocarbon production, we may often see one party unload responsibility onto another. In the 1920s, this was not the case, as we see from the poignant example of the Goose Creek oil field [*Poland and Davis*, 1969]. The Gaillard peninsula, located at the mouth of Goose Creek and overlying part of the oil field, began to settle and was soon covered by the waters of San Jacinto Bay. By 1925, maximum subsidence had exceeded 1 m and the area affected was about 4 km long and 2.5 km wide, approximately consistent with the boundary of the producing wells. The State of Texas claimed title to the lands submerged by the subsidence and sought to recover the value of oil removed after the submergence. The court, however, decided in favor of the defendants, accepting their contention that the subsidence was not the result of a natural process but generated by an act of man, namely the removal of large volumes of fluids and sand from the underground "No act of man can operate to deprive another man of his property under the law." If the subsidence had been a natural process, "an act of God," then presumably title to the submerged land and the underlying reserves would have passed to the state of Texas. Who today would plead in court to demonstrate his own responsibility in causing land subsidence?

Quantitatively speaking, the principle of effective intergranular stress advanced by *Terzaghi* [1923] gave great impulse to the theory viewing soil consolidation as the primary cause of land settlement. Soon, this principle was recognized as being an active factor in the compaction of an aquifer (the Dakota Sandstone) by *Meinzer and Hard* [1925], who stated that the overburden pressure of all beds above the confined Dakota aquifer was supported partly by the fluid pressure and partly by the sandstone itself, via the effective intergranular stress. They concluded that the grain-to-grain load had increased by about 50% because of the decline of artesian head. Based on both laboratory tests and field measurements, *Meinzer* [1928] cited evidence indicating the compressibility and elasticity of artesian aquifers. He recognized that water withdrawn

from storage was released by compression of the aquifer and by expansion of the water and that reduction of storage (compression) may be permanent (anelastic) as well as elastic. In the same year, *Russell* [1928] estimated that the anthropogenic subsidence of the land surface in eastern South Dakota due to the artesian head decline was at least 5 cm. Quite interestingly, he made this estimate without direct measurements of the settlement or calculation of the aquifer compaction. Based on the known quantity of water pumped out of the Dakota Sandstone in 15 years, which was equal to a layer of water 2 inches thick, he inferred that the area must have subsided by the same quantity. *Rappleye* [1933] provided the first specific records of subsidence due to groundwater pumping in the Santa Clara Valley (CA), and *Ingerson* [1941] described the subsidence in the Delano-Tulare-Wasco (CA) area by presenting a map and profiles of land subsidence based on comparison between leveling surveys performed in 1902, 1930, and 1940. By this time, the relationship between the removal of subsurface fluid (water, oil, and gas) and land subsidence was clear enough, at least in the USA. *Jacob* [1940] postulated that when water is pumped out from an elastic artesian aquifer system and pore pressure is decreased, withdrawn water is derived from water expansion, aquifer compression, and compression of the adjacent and intervening clay beds. He stated that the third source is probably the chief one: "because of the low permeability of the clays (or shales) there is a time lag between the lowering of pressure within the aquifer and the appearance of that part of water which is derived from storage in those clays (or shales)." Subsequently, *Lohaman* [1961] developed an equation for determining the amount of elastic compression of artesian aquifers from known declines in artesian pressure and hydromechanical properties of the aquifers. This compression was intended as being transferred to the ground surface, producing an estimate of the resulting land subsidence.

In the late 1950s and 1960s, the concept interrelating land subsidence and fluid withdrawal was universally accepted, thanks to the fundamental contributions by Poland, a pioneer in anthropogenic land subsidence studies [*Poland*, 1958, 1960, 1961; *Poland and Davis*, 1956, 1969; *Poland et al*., 1959; *Poland and Green*, 1962]. Around the same time, the principle of effective stress was universally recognized in geomechanics [*Taylor*, 1948; *Terzaghi and Peck*, 1948; *Leonards*, 1962]. *Mitchell* [1962] studied components contributing to pore pressure in clays and concluded that: "the effective stress principle and information obtained through the water pressure measurements correlate well with observed behavior of many fine-grained soils."

By the end of the 1960s, the concept and the mechanism underlying land subsidence of anthropogenic origin were clear. The way was open to new progress in the mathematical formulation of equations governing the process and corresponding solutions helpful in predicting expected land subsidence in exploited aquifer systems. This progress was greatly enhanced by the parallel development of computer technology.

A second important geomechanic effect associated with groundwater pumping from unconsolidated sedimentary aquifer systems is ground rupture. The nature of ground failure may range from fissuring, i.e., formation of an open crack, to faulting, i.e., differential offset of the opposite sides of the failure plane. Ground ruptures associated with land subsidence were first observed in 1949, in central Arizona, by *Feth* [1951]. In the wake of this pioneering work, it would take more than 20 years for the U.S. Geological Survey to undertake major investigations in subsiding areas of the southwestern United States (California, Arizona, Texas, and Nevada), where earth fissures had become a widespread problem [*Holzer*, 1976; *Holzer et al*., 1979; *Jachens and Holzer*, 1979; *Holzer and Pampeyan*, 1981; *Jachens and Holzer*, 1982].

Holzer and Pampeyan [1981] recognized that "the areal and temporal association of earth fissures with land subsidence caused by groundwater withdrawal indicated that these fissures were man induced." The underlying mechanism was highlighted at that time, as soon as enough field data became available to test the hypothesis. Bending caused by localized differential displacements was originally proposed by *Feth* [1951] to explain the observed fissuring. He speculated that it might have been caused by tensile strains generated by locally varying degrees of subsidence. He attributed the differential subsidence to abrupt variations in aquifer thickness. *Lofgren* [1971] conjectured that horizontal displacements measured in subsiding areas might be due to horizontal seepage forces. Based on the association of earth fissures with water table decline and other field evidence suggesting fissures formed at depth and propagated upward, *Holzer and Davis* [1976] held that fissures were caused by desiccation due to water table lowering. *Bouwer* [1977] suggested that earth fissures were caused by a rotation of rigid labs of overburden in response to regional differential subsidence. Only over the last decade has the availability of three-dimensional geomechanical models allowed for preliminary attempts at simulating ground ruptures as they relate to anthropogenic alterations in the porous medium stress state.

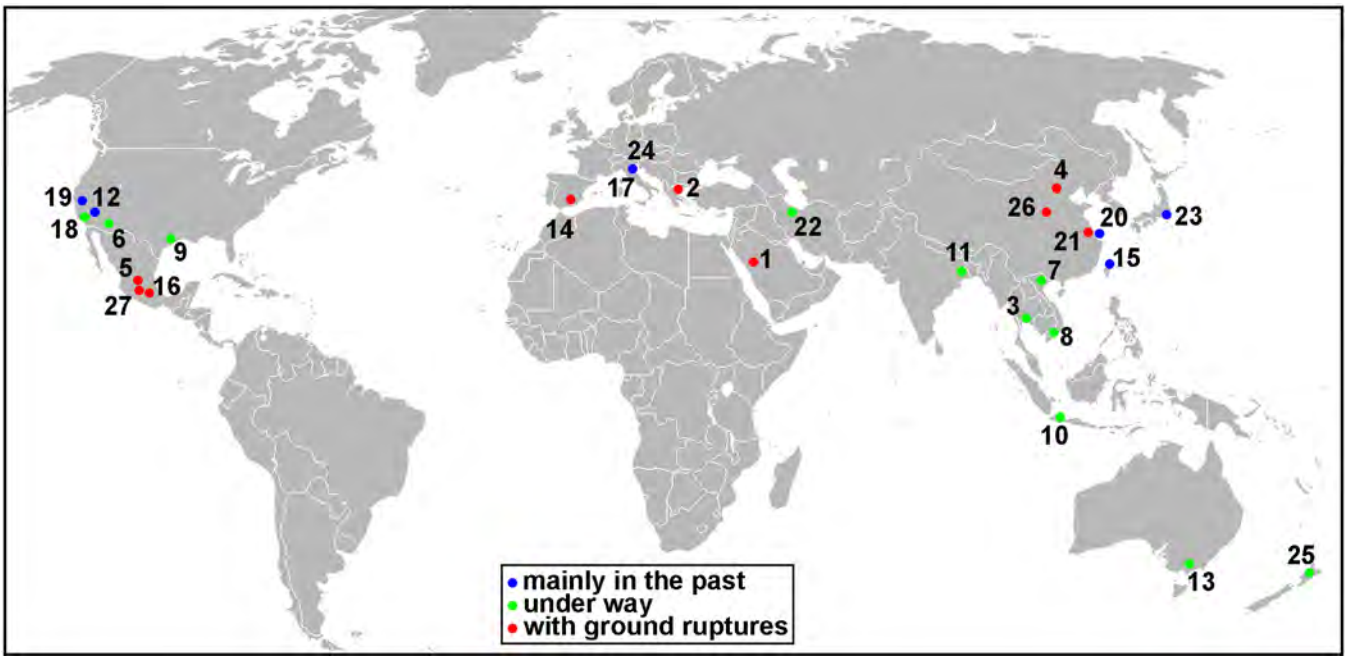

Figure 1. Major worldwide areas of anthropogenic land subsidence due to groundwater withdrawal. Different symbols are used to distinguish cases of subsidence (i) occurring mainly in the past, (ii) still under way, and (iii) associated with ground rupture. 1: Wadi Al-Yutamah, Saudi Arabia; 2: Anthemountas Basin, Greece; 3: Bangkok, Thailand; 4: Beijing, P. R. China; 5: Celaya, Mexico; 6: Eloy Basin, Arizona; 7: Hanoi, Vietnam; 8: Ho Chi Minh, Vietnam; 9: Houston, Texas; 10: Jakarta, Indonesia; 11: Kolkata, India; 12: Las Vegas, Nevada: 13: Latrobe Valley, Australia; 14: Lorca, Spain; 15: Taipei, Taiwan; 16: Mexico City, Mexico; 17: Ravenna, Italy; 18: San Joaquin Valley, California; 19: Santa Clara Valley, California; 20: Shanghai, P. R. China; 21: Su-Xi-Chang area, P. R. China; 22: Tehran, Iran; 23: Tokyo, Japan; 24: Venice, Italy; 25: Wairakei, New Zealand; 26: Xian, P. R. China; 27: Zamora de Hidalgo, Mexico City.

3. Land Subsidence Due to Groundwater Withdrawal

3.1. The Occurrence

Land subsidence is perhaps the most widespread and threatening geomechanical consequence of groundwater pumping. To be of major concern, groundwater withdrawal must occur in densely populated and highly developed areas, possibly located close to the sea or a lagoon or a delta, and take place from unconsolidated geological basins of alluvial, lacustrine, or shallow marine origin, formed typically, although not exclusively, in the Quaternary period. Quite often, especially at the onset of the occurrence, land settlement goes unnoticed, only to be discovered later on, when severe damage has already taken place. At this stage, undertaking effective remedial measures to mitigate the associated environmental and socioeconomical impact may prove tremendously expensive. However, in recent times, our awareness concerning the damage threatened by potential anthropogenic land subsidence has significantly grown at both the political and the general public level, thus contributing to lower the alarm threshold. As a major result, the most recent plans for subsurface resource development usually include a study of the related environmental impact presenting, wherever appropriate, numerical predictions of the expected land settlement above (and close to) the exploited system.

Figure 1 shows the areas of major anthropogenic land subsidence due to groundwater extraction worldwide. Table 1 gives the most significant records of the occurrences depicted in Figure 1. The maximum recorded settlement of all times amounts to more than 14 m, and was due to geothermal water production at Wairakei geothermal field, New Zealand [*Allis et al*., 2009] (Figure 2a). However, settlement depths approaching 10 m are not unusual (e.g., S. Joaquin Valley, CA, USA [*Galloway and Riley*, 1999] and Mexico City, Mexico [*Figueroa-Vega*, 1984; *Ortiz-Zamora and Ortega-Guerrero*, 2010]). The depth of fluid abstraction wells may range from those tapping very shallow water table aquifers quite close to the ground surface, to those tapping very deep (4000–5000 m) gas/oil reservoirs. The overall extent of the sinking area can be wide, totaling as much as 13,500 km^2 in the S. Joaquin Valley [*Poland and Lofgren*, 1984] and 12,000 km^2 in the Houston-Galveston area, Texas [*Gabrysch and Neighbors*, 2000], where groundwater was intensively withdrawn. China is perhaps the country with the largest cumulative area (about 80,000 km^2) where anthropogenic land subsidence primarily due to subsurface water overdraft has occurred [*Xue et al.,* 2005]. For an

Table 1. Selected Areas of Major Land Subsidence Due to Groundwater Withdrawal Worldwide[a]

No.	Location	Maximum Subs. (m)	Recent Subs. Rate (cm/yr)	Depth of Pumping (m)	Area of Subs. (km^2)	Principal References
1	Wadi Al-Yutamah	0.3 (1993–1996)		0–150	150	*Bankher and Al-Harthia* [1999]
2	Anthemountas Basin		3.5 (1995–2001)	30–150	40	*Raspini et al.* [2013]
3	Bangkok	2.1 (1933–2002)	2 (2005–2010)	30–300	700	*Phien-wej et al.* [2006] and *Aobpaet et al.* [2013]
4	Beijing	1.1 (1955–2007)	5 (2003–2010)	20–400	4,200	*Zhang et al.* [2014] and Zhu et al. (submitted manuscript, 2014)
5	Celaya	3.1 (1985–2008)	9 (2007–2011)	50–200	50	*Huizar-Álvarez et al.* [2011] and *Chaussard et al.* [2014]
6	Eloy Basin	3.0 (1948–1977)	4 (2010–2014)	100–760	1,000	*Holzer et al.* [1979] and *Conway* [2014]
7	Hanoi	0.5 (1988–2003)	7 (2007–2011)	0–80	35	*Thu and Fredlund* [2000] and *Dang et al.* [2014]
8	Ho Chi Minh	0.4 (1996–2005)	4 (2006–2010)	50–240	250	*Erban et al.* [2014]
9	Houston	3 (1915–2000)	2.5 (2005–2012)	60–900	12,000	*Gabrysch and Neighbors* [2000] and *Yu et al.* [2014]
10	Jakarta	4.1 (1974–2010)	26 (2007–2011)	40–240	660	*Ng et al.* [2012]
11	Kolkata	1.1 (1956–2000)	4 (2001–2005)	50–160	150	*Shau and Sikdar* [2011]
12	Las Vegas	2 (1935–2000)	2.5 (1997–1999)	200–300	250	*Amelung et al.* [1999] and *Hoffmann et al.* [2001]
13	Latrobe Valley	1.3 (1960–1977)	1.5 (2006–2011)	0–150	400	*Gloe* [1984]
14	Lorca	2.2 (1992–2012)	16 (1992–2011)	50–300	140	*González et al.* [2012]
15	Taipei	2 (1955–1991)	−0.7 (1989–2003)	50–250	200	*Chen et al.* [2007]
16	Mexico City	13 (1960–present)	30 (2007–2011)	0–350	250	*Ortiz-Zamora and Ortega-Guerrero* [2010] and *Chaussard et al.* [2014]
17	Ravenna	1.4 (1897–2002)	0.2 (1998–2002)	80–450	400	*Teatini et al.* [2006]
18	San Joaquin Valley	10 (1930–present)	30 (2007–2011)	60–600	13,500	*Galloway and Riley* [1999] and *Borchers and Carpenter* [2014]
19	Santa Clara Valley	4.3 (1910–1995)	−0.5 (1992–2000)	50–280	500	*Schmidt and Burgmann* [2003] and *Borchers and Carpenter* [2014]
20	Shanghai	2.6 (1958–2002)	1.5 (2006–2011)	10–330	5,000	*Wu et al.* [2010] and *Dong et al.* [2014]
21	Su-Xi-Chang area	1.1 (1960–1995)	3 (2003–2008)	20–200	4,000	*Shi et al.* [2007] and *Yu et al.* [2009]
22	Tehran	3.0 (1989–2004)	15 (2004–2005)	20–100	500	*Mahmoudpour et al.* [2013]
23	Tokyo	4.3 (1900–1975)	−0.3 (1991–2005)	0–400	3,400	*Sreng et al.* [2011]
24	Venice	0.12 (1952–1973)	0.1 (2008–2011)	70–350	150	*Gambolati et al.* [1974] and *Teatini et al.* [2012]
25	Wairakei	14.5 (1950–present)	9 (2000–2007)	250–800	25	*Allis et al.* [2009]
26	Xian	2.3 (1959–1995)	11 (2005–2012)	50–370	240	*Zhao et al.* [2008] and *Qu et al.* [2014]
27	Zamora de Hidalgo		18 (2007–2011)	0–300	15	*Chaussard et al.* [2014]

[a]The time of occurrence is provided between parentheses. Rates represent the local maximum measured rate for the specified period. Negative values mean uplift.

initial review of human-induced land subsidence through illustrative case histories worldwide and more recently from across the United States, the reader may consult *Poland* [1984] and *Galloway et al*. [1999], respectively.

The mechanism by which rock deforms and compacts under the influence of a fluid head change is well understood. The total geostatic load acting on the aquifer and confining beds is balanced by the pore pressure and the effective vertical and horizontal stresses. The introduction of a pumping well into a natural fluid flow system produces a disturbance that propagates its effect in space and time through the geological medium. Around the well, a cone of depression in the fluid head in the pumped formation develops and expands laterally, and to a minor extent also vertically. Both the intensity of the head drop at any point of the porous medium and the time lag between the inception of withdrawal and the arrival of the effect at that point, depend on the distance between the point and the well field, on the geometric and geologic configuration of the subsurface basin, on its boundary conditions, and on the fluid-dynamic and geomechanical properties of both fluid and formation: specifically, fluid density and viscosity and intrinsic medium permeability, porosity, and compressibility. Compressibility plays a major role in the resulting medium deformation. As the fluid head declines, pore pressure declines as well, and can no longer support as large a percentage of the load from overlying formations. Therefore, more of this load must now be borne by the grain-to-grain contacts of the geological material itself, with a stress transfer from the fluid to the solid phase, and a consequent increase in effective stress in both the pumped units and the adjacent formations (i.e., intervening aquitards and confining beds) which are progressively drained, and hence compact, with the amount of compaction primarily related to the compressibility of the compacting layers. The resulting cumulative compaction of subsurface layers extends its effect to the ground surface, which therefore subsides.

Let us compare anthropogenic land subsidence over gas/oil fields to that occurring over multiaquifer systems. Due to stress/strain redistribution in the thick overburden separating the reservoir from the earth's surface, settlement above gas/oil fields is typically lesser with respect to reservoir compaction, but it spreads over an area extending beyond the field itself. Conversely, aquifer systems are generally shallower and have a much larger areal extent than gas/oil fields. In these systems, sediment compaction is not contrasted by overlaying deposits and simply migrates toward the ground. Hence, such stratified systems behave

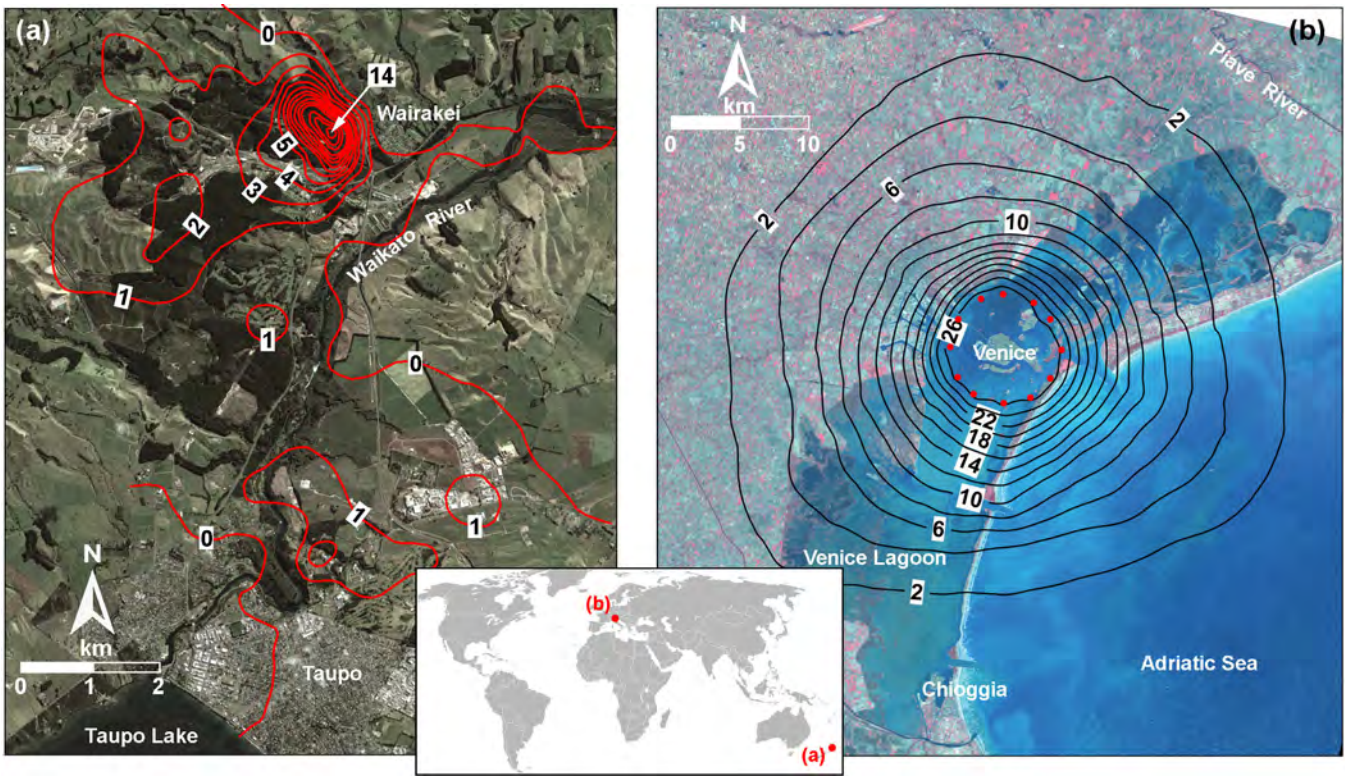

Figure 2. (a) Total subsidence at the Wairakei geothermal field over the 1953–2005 period. Contourline interval: 1 m; maximum subsidence contourline: 14 m [after *Allis et al*., 2009]. (b) Predicted uplift (cm) at Venice after 10 years of injection into the saline aquifers 650–1000 m deep below the lagoon. The injection wells are marked in red [after *Teatini et al*., 2011a].

mechanically as if they were 1-D structures, and, although fluid flow may be 3-D (to give a simple example, vertical in the confining beds and aquitards, and horizontal in the aquifers), land displacement occurs mostly in the downward vertical direction, and particularly so in multiaquifers with a high fraction of intervening clayey layers and/or a distributed pumping from a number of wellbores. In addition to dimensionality, other factors differentiate the mechanism of gas/oil field compaction from that of aquifer/aquitard compaction. Usually, both subsurface environments consist of a sequence of sands and clays (aquifer systems), and sandstones and shales (gas/oil reservoirs). Sandstones are cemented sands, whereas shales are clays that have undergone extensive mineralogical changes in the burial process associating them with hydrocarbon-bearing strata. These changes may have profoundly affected the shales compaction properties. Most freshwater aquifer systems are normally consolidated and normally pressurized, or only slightly overpressurized, and may lack important faults due to the typical formation mechanism involving a depositional alluvial/marine environment without significant interfering tectonic movements. However, their geomechanical simplicity may be partially offset by a lithostratigraphic complexity related to the distribution of clayey, silty, and sandy soils within the compacting system. It is well known that clay may be up to 2 orders of magnitude more compressible than sand at shallow depth [*Chilingarian and Knight*, 1960]. Hence, land subsidence of a freshwater system highly depends on the clayey and silty fraction within the system formed by confining beds, intervening aquitards, and interbedded lenses. Moreover, drainage from these beds can lag behind drainage from the producing sand, thus causing a delayed land subsidence which may manifest itself after wells shut down. In contrast, in deeply seated gas/oil fields, clay (shale) and sand (sandstone) tend to exhibit the same mechanical properties irrespective of lithology [*Finol and Sancevic*, 1995; *Baú et al*., 2002; *Ferronato et al*., 2013], which further differentiates the occurrence above pumped aquifer systems from that above productive gas/oil fields. For an interesting overview of the link between anthropogenic land subsidence and the actual mechanics of gas/oil reservoir compaction as perceived by oil industry, see *Doornhof et al*. [2006].

When a porous body experiences a change in the internal flow and stress fields, due, for example, to a sedimentation process producing a total stress increase, or to fluid pumping which causes a decrease in pore

pressure, the incremental effective stress and the fluid-dynamic gradient that develop are intimately connected. This connection was first recognized by *Biot* [1941], who developed the coupled theory of consolidation (and hence the coupled theory of land subsidence) where flow and stress are intimately connected. It states that fluid flow influences the porous mediums deformation, which in turn affects the flow field. Groundwater hydrologists, who are mainly concerned with the fluid-dynamic aspects of this coupled interrelation, have advanced the uncoupled theory of flow, based on the so-called diffusion equation. *Theis* [1935] solved the single-phase flow of groundwater by incorporating the rock structural properties into a lumped geomechanical parameter (i.e., the elastic storage coefficient S_s defined in the next section). Theis' solution to the diffusion equation is calculated separately, independently of the medium structural solution, in order to provide the pore pressure distribution. Once obtained, the pore pressure is used as the external driving force in predicting the medium deformation: in particular, the vertical displacement at the ground surface, that is, land subsidence.

In summary, a realistic uncoupled representation of the mechanism of anthropogenic land subsidence due to groundwater withdrawal involves a two-step process. The first step addresses the fluid-dynamic part of the occurrence, where the substantial impact of the geomechanical porous mediums flow behavior may be quite effectively accounted for by the elastic storage S_s. The second step solves the structural problem by using the fluid pore pressure p (or better, its spatial gradient) distribution calculated in the first step as a driving force within the medium (possibly over or under consolidated and faulted) in order to provide the solid skeleton deformation and subsidence (i.e., vertical displacement) at land surface.

Four factors may partially combine to produce measurable settlement records [*Gambolati et al.*, 2005]:

1. Shallow burial depth of the pumped formations;

2. Highly compressible deposits laid down in alluvial or shallow marine or lacustrine environments;

3. Considerable pore pressure decline; and

4. Large thickness of the depressurized water-bearing strata.

Unless the aquifers are overpressurized, factors 1 and 3 are mutually exclusive, while they can both be associated with factors 2 and 4. For a large subsidence to occur, however, a soft compacting rock is needed, and/or a large pressure drawdown. To give a few examples, Mexico City sank by 10 m with a maximum pressure decline of only 0.7 MPa because of the extremely soft high-porosity soils of the compacting shallow formations located within the upper 50 m [*Rivera et al.*, 1991], while the 9 m and the 6.7 m settlement reported from the Wilmington [*Rintoul*, 1981] and Ekofisk [*Hermansen et al.*, 2000; *Zaman et al.*, 1995] oil fields, CA, USA and the North Sea, Europe, respectively, are due to the pronounced pore pressure drop (exceeding 20 MPa in the latter) combined with the considerable thickness of the compacting units. Although land subsidence above hydrocarbon fields is outside the scope of the present paper, it is perhaps worth mentioning that at Ekofisk the reservoir rock has exhibited a sudden increase in compressibility at some stage of the field development, with a large irreversible deformation defined as "pore collapse," believed to be the main reason for the unexpected large settlement over the field [*Zaman et al.*, 1995].

Some aquifers may be overconsolidated [*Holzer*, 1981]. Overconsolidation tends to reduce the early subsidence rate and then generate a sudden unexpected growth at some stage of extraction when the effective stress exceeds the preconsolidation stress. If the water or gas/oil-bearing sediments are preconsolidated it may be very difficult to predict anthropogenic land subsidence prior to the field/aquifer development. A preconsolidation effect might have been caused in the geological past by uplift followed by erosion of the sediments overlying the fluid-bearing layers, by fluid overpressure, or both. The aforementioned processes led to a reservoir/aquifer system expansion much slighter than the original, virgin, mostly unrecoverable compaction. When pore pressure drops due to fluid removal, a reloading of the pumped formations takes place. Initially, compaction is slight, and thus, land settlement is as well. However, as soon as the maximum experienced load is surpassed, rock compression occurs on the virgin loading curve with a sudden increase in compressibility and in the resulting subsidence rate. Another factor that may influence the occurrence is the presence of faults within the developed system and the overburden, as in the case of Las Vegas, NE, USA [*Amelung et al.*, 1999]. Faults may weaken the porous medium structure and make both analysis and prediction more difficult.

The analysis and prediction of expected anthropogenic land subsidence due to fluid pumping require a careful reconnaissance study of the area of interest, with a detailed layout of the basins geology and

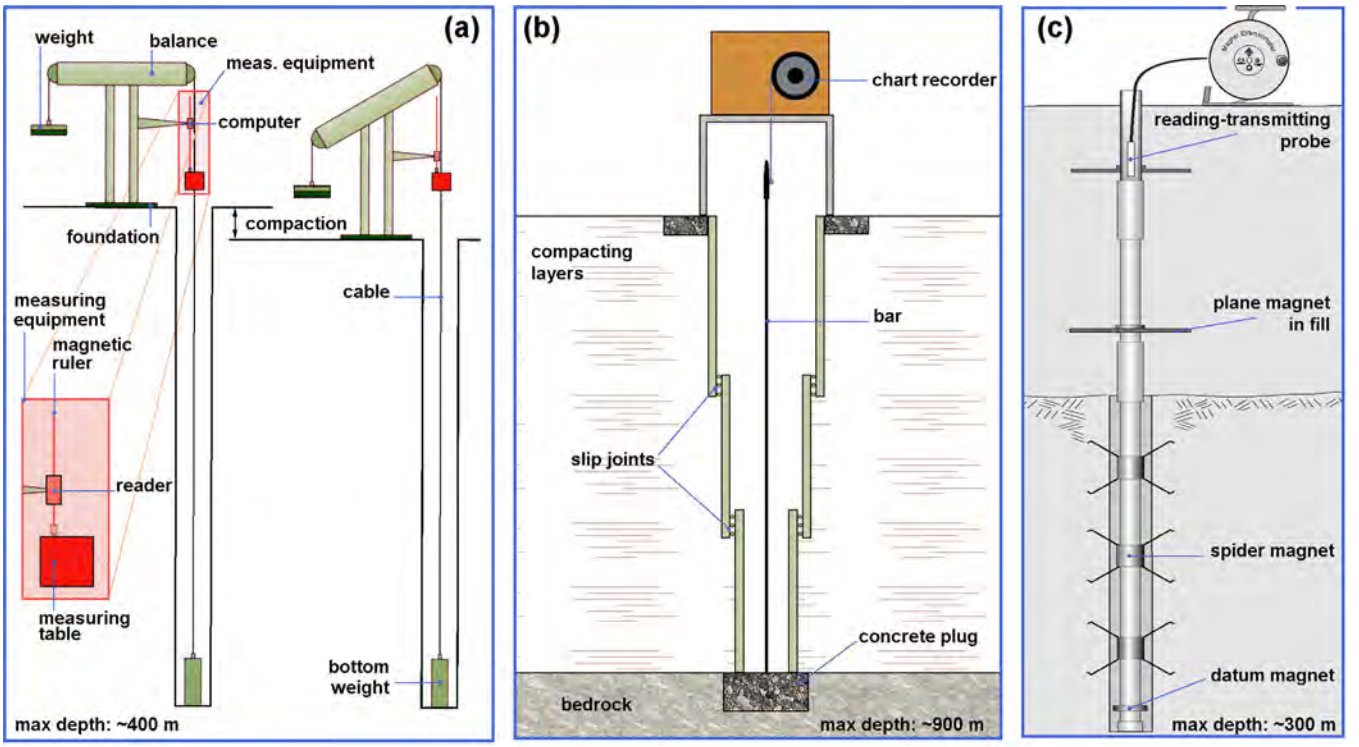

Figure 3. Schematic representation of single-layer (a) cable and (b) slip-joint casing extensometers. A multilayer magnetic borehole extensometer used to record the deformation of aquifer-aquitard systems is sketched in Figure 3c.

geometry and reconstruction of the pumping rate evolution, pressure head, and displacements of the land surface. Geomechanical and hydraulic properties are of the utmost importance. Preconsolidation stress, zones of overpressure, and faults/thrusts in their extent, orientation and geomechanical properties (i.e., friction angle and cohesion) must all be reliably identified. Advanced technology (2-D and 3-D seismic surveys, airborne-electromagnetic investigations, well-logs, exploration boreholes, pumping tests, laboratory analyses) can be of great help. Much progress has also been made since the traditional spirit leveling, in accurately monitoring ground surface movements. New techniques include DGPS (Differential Global Positioning System) and InSAR (Interferometric Synthetic Aperture Radar), by which land subsidence is measured from space with very high precision (see section 6). Advances have also been accomplished in measuring shallow and deep aquifer system compaction by single-level cable (Figure 3a) and multilevel magnetic (Figure 3b) borehole extensometers. Anthropogenic land subsidence modeling and forecasting tools are continuously improved. They take advantage of both enhanced computer devices (e.g., parallel hardware) and advanced measurements technology applied to horizontal and vertical ground movements (e.g., DGPS and InSAR technologies). Modeling tools are helpful in determining and distinguishing among multiple causes, and can be effectively combined with measurement techniques. Once the models have been calibrated upon the observed history of the aquifer they can be used in their predictive capacity in various scenarios of groundwater use, thus helping to develop integrated resource management programs that would hopefully take into account environmental and socioeconomic impacts. The models are used to evaluate the adverse consequences of fluid extraction in a medium/long-time range, in particular for urban flood management of coastal areas and in other cases of environmental vulnerability.

For the sake of completeness, we should mention other types of anthropogenic land subsidence that are not addressed by the present analysis. Most of them are less important in terms of socioeconomic and environmental impact. They include underground mining, carbonate rock solution, subsurface erosion, surface loading, land drainage and reclamation, histosoil (peat) oxidation, dissolution of soil carbon, and water application [*Allen*, 1984]. As an example of land subsidence due to peat oxidation, see the recent paper by *Zanello et al*. [2011].

3.2. Basic Principles and Equations

As outlined above, it has long been understood that land subsidence is best analyzed according to the theory of consolidation [*Biot*, 1941, 1955], which holds that consolidation itself represents the response of a compressible porous medium to changes in the flow field operating within it. A complete analysis of land subsidence requires determination of the 3-D deformation field accompanying the 3-D flow field, and must be accomplished in a complex multiaquifer system. A few basic principles underlie the consolidation process. The first principle, advanced by *Terzaghi* [1923], states that the total stress σ_{tot} acting in any point of the porous medium is equal to the sum of the effective intergranular stress σ_{eff} and the neutral pore pressure p

$$\sigma_{tot} = \sigma_{eff} + p.$$

Deformation of the porous body is controlled exclusively by variation of the effective stress σ_{eff}. If we consider changes relative to an initial undisturbed state of equilibrium, the Cauchy equations of equilibrium are cast in terms of incremental effective stress and pore pressure, and read:

$$\begin{aligned} \frac{\partial \sigma_{xx}}{\partial x} + \frac{\partial \tau_{xy}}{\partial y} + \frac{\partial \tau_{xz}}{\partial z} &= \frac{\partial p}{\partial x} \\ \frac{\partial \tau_{yx}}{\partial x} + \frac{\partial \sigma_{yy}}{\partial y} + \frac{\partial \tau_{yz}}{\partial z} &= \frac{\partial p}{\partial y} \\ \frac{\partial \tau_{zx}}{\partial x} + \frac{\partial \tau_{zy}}{\partial y} + \frac{\partial \sigma_{zz}}{\partial z} &= \frac{\partial p}{\partial z} \end{aligned} \tag{1}$$

where σ_{xx}, σ_{yy}, and σ_{zz} are the incremental normal effective stresses along the coordinate directions x, y, and z and $\tau_{xy} = \tau_{yx}$, $\tau_{xz} = \tau_{zx}$, and $\tau_{yz} = \tau_{zy}$ are the incremental shear stresses.

The relationships between the incremental effective stress tensor σ and the incremental strain tensor ϵ for a geomechanical isotropic medium read:

$$\begin{bmatrix} \sigma_{xx} \\ \sigma_{yy} \\ \sigma_{zz} \\ \tau_{xy} \\ \tau_{xz} \\ \tau_{yz} \end{bmatrix} = D^{-1} \begin{bmatrix} \epsilon_{xx} \\ \epsilon_{yy} \\ \epsilon_{zz} \\ \epsilon_{xy} \\ \epsilon_{xz} \\ \epsilon_{yz} \end{bmatrix} \tag{2}$$

with matrix D^{-1} equal to:

$$D^{-1} = \frac{E}{(1+v)(1-2v)} \begin{bmatrix} 1-v & v & v & 0 & 0 & 0 \\ v & 1-v & v & 0 & 0 & 0 \\ v & v & 1-v & 0 & 0 & 0 \\ 0 & 0 & 0 & \frac{1-2v}{2} & 0 & 0 \\ 0 & 0 & 0 & 0 & \frac{1-2v}{2} & 0 \\ 0 & 0 & 0 & 0 & 0 & \frac{1-2v}{2} \end{bmatrix} \tag{3}$$

where E and v are the rock Young modulus and the Poisson ratio, respectively. Typically, in layered aquifer systems laid down in a depositional environment, the geomechanical properties along the vertical direction are different from those in a horizontal direction. The geomechanical properties of a transversally isotropic porous medium are fully described by five independent parameters: E_v, E_h, v_v, v_h, G_v. G_h is dependent on E_h and v_h through the well-known equation:

$$G_h = \frac{E_h}{2(1+v_h)} \tag{4}$$

Thermodynamic consistency requires the positive definiteness of matrix C^{-1} relating the stress tensor to the strain tensor, which implies [*Ferronato et al.*, 2013]:

$$1-\nu_h^2 > 0 \text{ and } 1-\nu_h-2\nu_h^2\frac{E_v}{E_h} > 0.$$

Setting,

$$\begin{aligned} \vartheta &= \frac{E_h}{E_v} \\ \eta &= \frac{E_h}{2(1+\nu_h)G_v} \\ \alpha &= \frac{1}{E_v}\left(1-\frac{2\nu_v^2}{1-\nu_h}\frac{E_v}{E_h}\right), \end{aligned} \tag{5}$$

the constitutive matrix C^{-1} (equivalent to D^{-1} for a transversally isotropic medium) reads [*Ferronato et al.*, 2013]:

$$C^{-1} = \frac{1}{(1-\nu_h^2)\alpha}\begin{bmatrix} C_1^{-1} & 0 \\ 0 & C_2^{-1} \end{bmatrix} \tag{6}$$

where,

$$C_1^{-1} = \begin{bmatrix} \vartheta-\nu_v^2 & \nu_v^2+\vartheta\nu_h & \nu_v(1+\nu_h) \\ \nu_v^2+\vartheta\nu_h & \vartheta-\nu_v^2 & \nu_v(1+\nu_h) \\ \nu_v(1+\nu_h) & \nu_v(1+\nu_h) & 1-\nu_v^2 \end{bmatrix} \qquad C_2^{-1} = \frac{\vartheta(1-\nu_h)-2\nu_v^2}{2}\begin{bmatrix} 1 & 0 & 0 \\ 0 & 1/\eta & 0 \\ 0 & 0 & 1/\eta \end{bmatrix}$$

Written explicitly equation (6) takes on the form:

$$\begin{bmatrix} \sigma_{xx} \\ \sigma_{yy} \\ \sigma_{zz} \\ \tau_{xy} \\ \tau_{xz} \\ \tau_{yz} \end{bmatrix} = \frac{E_h E_v}{(1+\nu_h)[(1-\nu_h)E_h-2\nu_v^2 E_v]} \times \begin{bmatrix} \vartheta-\nu_v^2 & \nu_v^2+\vartheta\nu_h & \nu_v(1+\nu_h) & 0 & 0 & 0 \\ \nu_v^2+\vartheta\nu_h & \vartheta-\nu_v^2 & \nu_v(1+\nu_h) & 0 & 0 & 0 \\ \nu_v(1+\nu_h) & \nu_v(1+\nu_h) & 1-\nu_v^2 & 0 & 0 & 0 \\ 0 & 0 & 0 & \frac{\vartheta(1-\nu_h)-2\nu_v^2}{2} & 0 & 0 \\ 0 & 0 & 0 & 0 & \frac{\vartheta(1-\nu_h)-2\nu_v^2}{2\eta} & 0 \\ 0 & 0 & 0 & 0 & 0 & \frac{\vartheta(1-\nu_h)-2\nu_v^2}{2\eta} \end{bmatrix} \begin{bmatrix} \epsilon_{xx} \\ \epsilon_{yy} \\ \epsilon_{zz} \\ \epsilon_{xy} \\ \epsilon_{xz} \\ \epsilon_{yz} \end{bmatrix} \tag{7}$$

The coefficient α provided in equation (5) is the vertical oedometric compressibility of the medium prevented from expanding laterally [*Gambolati et al.*, 1984]. Setting $\nu_h = \nu_v$, $E_h = E_v$, $G_h = G_v$, equation (6) turns into equation (2) and α becomes:

$$\alpha = \frac{(1+\nu)(1-2\nu)}{(1-\nu)E} \tag{8}$$

i.e., the well-known vertical compressibility of an isotropic soil. If we replace the relations between the effective stress and the strain above into the Cauchy equations, we obtain the equilibrium equations for a porous medium subject to pore pressure variations p within it, written in terms of displacements (isotropic medium):

$$\begin{aligned} G\nabla^2 u + (\lambda+G)\frac{\partial \epsilon}{\partial x} &= \frac{\partial p}{\partial x} \\ G\nabla^2 v + (\lambda+G)\frac{\partial \epsilon}{\partial y} &= \frac{\partial p}{\partial y} \\ G\nabla^2 w + (\lambda+G)\frac{\partial \epsilon}{\partial z} &= \frac{\partial p}{\partial z} \end{aligned} \tag{9}$$

where u, v, and w are the components of the incremental position vector along the coordinate axes x, y, and z, respectively, ∇^2 is the Laplace operator, λ is the Lamè constant equal to $\nu E/[(1-2\nu)(1+\nu)]$, and $\epsilon = \epsilon_{xx}+\epsilon_{yy}+\epsilon_{zz}$ is the volume strain or dilatation. Similar equations hold for a transversally isotropic medium, not given here, however, because of their greater complexity. There are three equations with four unknowns: u, v, w, and p. The additional equation needed to close the system is provided by the groundwater flow equation that controls subsurface flow within the aquifer.

The flow equation is based on the principle of mass conservation for both solid grains and water. Thus, Darcy's law must be cast in terms of the relative velocity of fluid to grains. *Cooper* [1966] and *Gambolati* [1973a] derived the flow equations by assuming a grain velocity different from zero, and worked with material derivatives (total derivatives and substantial derivatives) in the appropriate places in the development. *Gambolati* [1973b] showed that the grain velocity can be discarded, i.e., assumed to be zero, as long as the final soil settlement does not exceed 5% of the original aquifer thickness, a condition reached in nearly all applications. *DeWiest* [1966] took into consideration the dependence of the hydraulic conductivity on the waters specific weight γ via the intrinsic permeability and the dependence of γ on the incremental pressure variation. *Gambolati* [1973b] again showed that the influence of the dependence of γ on the hydraulic conductivity is very slight, and can safely be neglected. Later, within this framework, the groundwater flow equation as originally developed by *Biot* [1941, 1955] was elegantly and clearly derived by *Verruijt* [1969], and thus the fourth equation to be added to the above equation (9) reads:

$$\frac{1}{\gamma}\nabla \cdot (K_{ij}\nabla) = n\beta\frac{\partial p}{\partial t} + \frac{\partial \epsilon}{\partial t} \tag{10}$$

with ∇ the gradient operator equal to $\partial/\partial x + \partial/\partial y + \partial/\partial z$, $K_{ij} = k_{ij}\gamma/\mu$ is the hydraulic conductivity tensor with principal components K_{xx}, K_{yy}, and K_{zz}, k_{ij} is the intrinsic permeability tensor, μ the viscosity of water, n the medium porosity, and β the compressibility of water. Equation (9) together with equation (10) forms the mathematical basis of the so-called "coupled" (or Biot) formulation of flow and stress in an isotropic porous medium experiencing a groundwater flow field. It is the most sophisticated theoretical approach to the simulation of land subsidence in the area of linear elasticity. *Gambolati* [1974] showed that in any point P of the porous medium, the deformation may be expressed as the sum of two contributing factors: (1) the pointwise deformation caused by the incremental pore pressure acting in P and (2) the deformation caused by the pressure p acting outside P, namely in the remainder of the medium. *Gambolati* [1974] called the second factor the "three-dimensional effect": it vanishes, of course, in one-dimensional media. The first factor is expressed as:

$$\epsilon = \frac{1}{E_v}\left(1 - \frac{2\nu_v^2}{1-\nu_h}\frac{E_v}{E_h}\right)p = \alpha p$$

in a geomechanical transversally isotropic medium, and

$$\epsilon = \frac{(1+\nu)(1-2\nu)}{(1-\nu)E}p = \alpha p$$

in a geomechanical isotropic medium, with α the vertical compressibility previously defined. Replace the above expression for ϵ in the flow equation (10) and you obtain the so-called "uncoupled" formulation of

flow and stress. In the uncoupled formulation the flow equation is solved for p independently of the stress equation, with the gradient of the pore pressure variations later integrated into the equilibrium equation (9) as a known external source of strength. The uncoupled flow equation thus reads:

$$\nabla\left(K_{ij}\frac{\nabla p}{\gamma}\right)=\gamma(n\beta+\alpha)\frac{\partial p}{\partial t} \tag{11}$$

Assuming the medium to be transversally isotropic as far as the hydraulic conductivity is concerned as well, having axes coincident with the principal directions of anisotropy, equation (11) becomes:

$$\frac{\partial}{\partial x}\left(K_{xx}\frac{\partial p}{\partial x}\right)+\frac{\partial}{\partial y}\left(K_{yy}\frac{\partial p}{\partial y}\right)+\frac{\partial}{\partial z}\left(K_{zz}\frac{\partial p}{\partial z}\right)=S_s\frac{\partial p}{\partial t} \tag{12}$$

The coefficient $S_s=\gamma(n\beta+\alpha)$ is the specific elastic storage coefficient referred to previously.

The uncoupled equation has been the basis of classical groundwater hydrology from the very beginning of quantitative hydrogeology's development [e.g., *Theis*, 1935; *Jacob*, 1940; *Todd*, 1960; *Bear*, 1972], and is still universally used today. The superiority of the coupled approach in predicting land subsidence due to groundwater pumping has been disputed by *Gambolati et al*. [2000], who showed that the uncoupled pressure solution can be safely used in predicting land subsidence in compacting sedimentary basins, the coupled and the uncoupled solution being virtually indistinguishable at any time of practical interest.

Is may also be of interest to mention some basic definitions of oedometer vertical soil compressibility, which is the main rock parameter controlling land subsidence. The definition of α given above is the one derived from the classical theory of elasticity assuming reversible elastic properties of the porous medium. The problem of defining various rock compressibilities is thoroughly discussed by *Zimmerman* [1991]. In the present analysis, we restrict our discussion to the comparison between α as defined above, and the compressibility c_b as is typically defined in geotechnique. In the laboratory, geotechnicians define and measure the following compressibility for aquifer/aquitard soil samples:

$$c_b=\frac{de}{dp}\frac{1}{1+e} \tag{13}$$

with $e=n/(1-n)$ the soil void ratio. Assume a 1-D soil sample with initial length Δz experiencing a vertical (oedometer) deformation $\delta(\Delta z)$. In the classical elastic theory, the vertical compressibility α is defined as:

$$\alpha=\frac{\delta(\Delta z)}{\Delta z}\frac{1}{p}=\frac{\epsilon}{p} \tag{14}$$

where p, equal and opposite to the incremental effective stress, is negative in the sample compaction $\delta(\Delta z)$. Using the void ratio, we can write:

$$\delta(\Delta z)=[\Delta z+\delta(\Delta z)]\frac{e}{1+e}-\Delta z\frac{e_0}{1+e_0} \tag{15}$$

where e_0 is the initial void ratio prior to compaction (Figure 4).

Equation (15) assumes that the individual soil grains are incompressible, so that the sample volume $\delta(\Delta z)$ is equal to the variation of the porous volume (Figure 4). By dividing both sides of equation (15) by Δz and rearranging, we obtain:

$$\epsilon=\frac{\delta(\Delta z)}{\Delta z}=\frac{e-e_0}{1+e_0} \tag{16}$$

We also have:

$$\alpha=\frac{\epsilon}{p}=\frac{e-e_0}{p(1+e_0)}$$

and if α does not depend on p:

$$\frac{de}{dp}=\alpha(1+e_0) \tag{17}$$

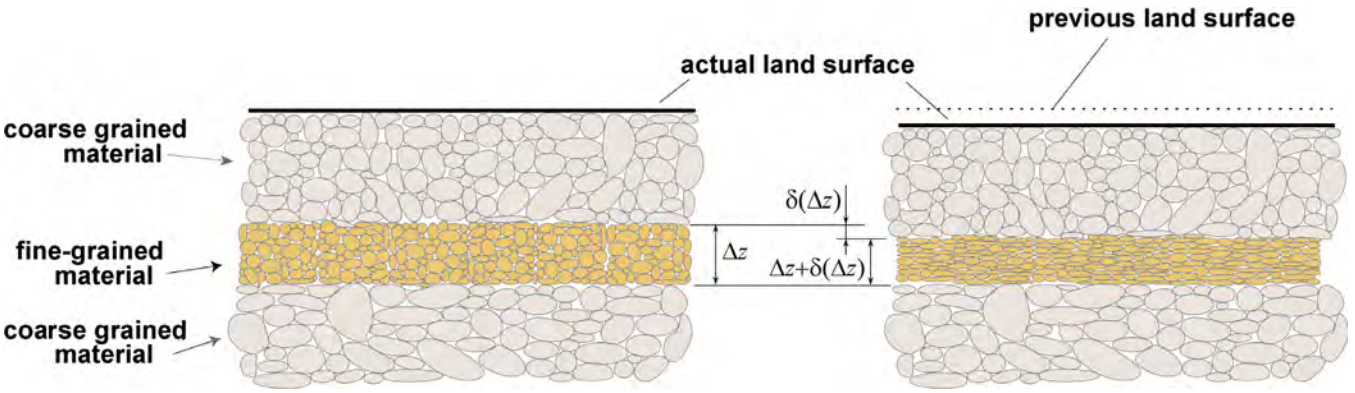

Figure 4. Soil compaction with a reduction of the porous space (grains are incompressible).

i.e., the void ratio is proportional to the incremental pressure p (for any given initial e_0). Substitution of equation (17) into (13) leads to:

$$c_b = \alpha \frac{1+e_0}{1+e} = \alpha \frac{1+e_0}{1+e_0+\alpha p(1+e_0)} = \frac{\alpha}{1+\alpha p}$$

Only when the incremental pressure p approaches 0, do α and c_b coincide. In general, the two compressibilities α and c_b are not equal and cannot be considered simultaneously constant. The expression of c_b versus ϵ is (from equation (16)):

$$c_b = \frac{1+e_0}{1+e}\frac{d\epsilon}{dp} = \frac{1}{1+\epsilon}\frac{d\epsilon}{dp} \tag{18}$$

If α is constant $d\epsilon/dp = \alpha$ and we have:

$$c_b = \frac{\alpha}{1+\epsilon} = \frac{\alpha}{1+\alpha p} \tag{19}$$

Gambolati [1973b] has shown that the assumption of constant α can be easily removed to give the general correct relationship between α and c_b:

$$c_b = \frac{p\frac{d\alpha}{dp}+\alpha}{1+\alpha p} \tag{20}$$

Should c_b be constant, equation (20) can be integrated to provide α:

$$\alpha = \frac{e^{pc_b}-1}{p} \tag{21}$$

The assumption that the individual grains are incompressible is fully warranted by the fact that the compressibility of any aquifer system is orders of magnitude greater than the compressibility of the single grain (*Geerstma* [1973] provides the value of $\alpha = 0.16\times10^{-5}$ bar^{-1} for grains of silicate). As an example, see in Figure 5 the behavior of α versus depth and vertical effective intergranular stress σ_{zz} in the sedimentary basin of the river Po plain, Italy [*Gambolati et al*., 1991, 1999; *Comerlati et al*., 2004]. However, as long as the ultimate relative compaction αp does not exceed 5% of the compacting unit (which is quite usual in real geologic formations, particularly in shallow formations), the difference between α and c_b does not exceed 2–3% [*Gambolati*, 1973b, Figure 14] and the two definitions are practically interchangeable.

Finally, it is worth mentioning that, when comprehensive in situ and lab soil characterizations are available, more realistic constitutive formulations taking into account plastic or viscoplastic behavior may be developed and used for the simulation and prediction of land subsidence in soft underconsolidated alluvial basins [e.g., *Ye et al*., 2012].

3.3. Modeling Land Subsidence

Schiffman et al. [1969] have attempted the first classification of consolidation theories (and hence of land subsidence), subdividing them into categories: (a) one-dimensional *Terzaghi* [1923] theory, (b) pseudo

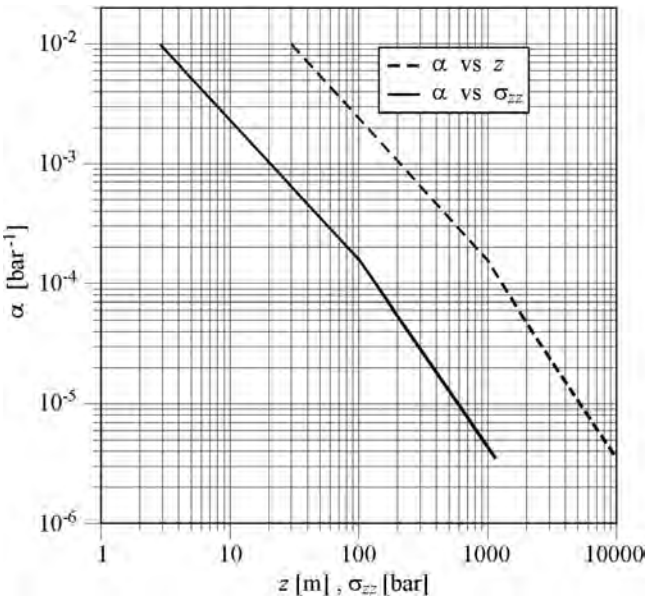

Figure 5. Uniaxial vertical compressibility α versus effective stress σ_{zz} and depth z in the Po river plain, Italy [after *Comerlati et al.*, 2004].

three-dimensional consolidation theory based on the diffusion equation, and (c) coupled three-dimensional consolidation theory based on the *Biot* [1941] equations. Actually, point (a) must be further divided into: (a_1) 1-D diffusion equation followed by 1-D vertical consolidation, and (a_2) 3-D or 2-D diffusion equation followed by 1-D pointwise consolidation. Each of the above modeling approaches implies approximations at a different level. For instance, category (a_1) is well suited for multiaquifer freshwater systems where the horizontal dimension is much larger, say orders of magnitude, than the vertical one. Under these circumstances at the regional-scale consolidation occurs mainly in the vertical direction, or rather, the deformation takes place as in a natural oedometer, with lateral expansion prevented and hence with $u \simeq v \simeq 0$. Category (b) is the uncoupled approach discussed above, and is correct in the vast majority of applications where consolidation occurs in the horizontal direction as well for any time of practical interest. Finally, a few special applications of consolidation may require the use of a fully coupled 2-D or 3-D model (dewatering, building foundations, overland man-made structures, etc.) where typically, the vertical size of the porous medium involved is in the same order of magnitude as the horizontal size [*Gambolati*, 1992]. We find another case where a coupled model may be helpful in the simulations of the Nordbergum effect [*Wolf*, 1970], namely the increase of pore pressure in confining beds overlying and/or underlying a pumped aquifer immediately after pumping inception. Usually this is a second-order effect that quickly dissipates as withdrawal proceeds. It has a negligible influence on the land subsidence soon after measurable compaction starts.

It goes without saying that the first models used to predict land subsidence caused by groundwater pumping were based on the 1-D *Terzaghi* [1923] theory. The models by *Domenico and Mifflin* [1965] and *Lofgren and Klausing* [1969] fall into this category. However, as early as 1960, *McNamee and Gibson* [1960] attempted to derive analytical solutions to the Biot consolidation of an isotropic porous medium for various sets of boundary conditions, and even earlier, *McCann and Wilts* [1951] had developed the first rudimental mathematical model of land subsidence over the oil field of the Long Beach-San Pedro area (CA) by simulating the oil reservoir with a set of hollow cavities (called "tension centers") strategically located within the field embedded in a linearly elastic semi-infinite porous medium so as to reproduce the land settlement measured overland. At the internal boundary of each cavity, a pore pressure decline was prescribed equal to the field pressure depletion. *McCann and Wilts* [1951] met serious difficulties in matching the observations, as their elastic cavities model was far from the physical and geometrical reality. Much closer to the actual physical setting was the tension center model developed by *Geerstma* [1966] and based on the theory of poroelasticity (the same as Biots). *Geerstma*'s [1966] tension center was infinitesimal and made from the same material as the reservoir. Land subsidence was predicted by numerically integrating *Geerstma*'s [1966] elementary solution over the depleted reservoir, allowing for a nonuniform pore pressure decline. *Geerstma*'s [1966] model represented a major breakthrough for the prediction of land subsidence over producing hydrocarbon fields. Its major limitation was the requirement of a geomechanically homogeneous and isotropic half-space embedding the reservoir, a condition rarely found in real-world applications. An improvement was contributed by *Gambolati* [1972], who extended *Geerstma*'s [1966] homogeneous solution to a heterogeneous tension center and showed that *McCann and Wilts* [1951] was a special case of his solution for an infinitely elastic tension center.

The first (numerical) model falling into category (a_2) above was developed by *Gambolati and Freeze* [1973] and *Gambolati et al.* [1974] to simulate and predict the land subsidence caused at Venice, Italy, by large groundwater withdrawals occurring in the 1950s and 1960s from a 300 m thick freshwater aquifer system.

The flow model was 3-D axisymmetrical solved by finite elements, while the land subsidence model was 1-D vertical with the center of the city as the reference location (Figure 6a). It took into consideration the unrecoverable clay and silt compaction in unloading as a consequence of the expected shutdown of the pumping wells. This implies using a different soil compressibility in loading and unloading, i.e., in depleting and recovering the aquifer system. Four years later, *Lewis and Schrefler* [1978] replicated the same simulation at Venice with a fully coupled consolidation model: with some small differences emerged due to the different parameters and boundary conditions implemented into their model.

The pioneering modeling study by *Gambolati and Freeze* [1973] opened the way to new more sophisticated models. *Helm* [1975] developed a 1-D aquifer compaction model of a multiaquifer system solved by finite differences using differing compressibility values for recoverable and unrecoverable compression. A second paper [*Helm*, 1976] allowed for the compressibility to be stress dependent. *Helm* [1984] also discussed various depth-porosity and aquitard-drainage models. Interbed storage changes in compacting aquifers were also considered, by *Leake* [1990]. The effect of viscosity was introduced in an aquifer model by *Corapcioglu and Brutsaert* [1977], while an integrated vertical 1-D subsidence equation was contributed by *Bear and Corapcioglu* [1981a]. *Gambolati et al*. [1991, 1999] and *Teatini et al*. [1995, 2006] (Figure 6b) applied finite models to predict anthropogenic land subsidence due to subsurface water withdrawals in a variety of 3-D regional settings of Northern Italy. Predictive numerical models have been developed for the majority of the main sites strongly affected by land subsidence over the last decades: Mexico City in Mexico [*Ortega-Guerrero et al*., 1999; *Ortiz-Zamora and Ortega-Guerrero*, 2010], Shanghai in China [*Shi et al*., 2007; *Ye et al*., 2012], Central Valley, Santa Clara Valley, and Antelope Valley in California [*Leake*, 1990; *Wilson and Gorelick*, 1996; *Leake and Galloway*, 2010], Houston in Texas [*Kasmarek and Strom*, 2002], Hanoi in Vietnam [*Thu and Fredlund*, 2000], and Tokyo in Japan [*Aichi*, 2008].

The formulation underlying the above models is generally an uncoupled one. Examples of coupled models, generally used to simulate schematic geologic systems, may be found in *Lewis and Schrefler* [1978], *Safai and Pinder* [1979, 1980], *Bear and Corapcioglu* [1981b], *Hsieh* [1996], and *Burbey and Helm* [1999]. *Fallou et al*. [1992] solved the coupled model by using an original perturbation technique.

At present, a certain number of numerical codes is available based on both finite differences and finite elements that can simulate and predict anthropogenic land subsidence due to fluid withdrawal in 3-D geological and geometrical settings. The codes operate according to elastic, elastoplastic, or visco-elastoplastic geomechanical constitutive laws and recur to even the most advanced parallel computer architectures, which enable them to deal with highly complex heterogeneous geologies and geometries. The codes most often used to simulate regional-scale land subsidence due to groundwater withdrawal are the MODFLOW-based packages IBS1 (Interbed Storage Package, version 1) [*Leake and Prudic*, 1991], IBS2 [*Leake*, 1990], and SUB-WT [*Leake and Galloway*, 2007]. All these packages fall into category (a), defined above. For a review of the principal features of the MODFLOW-based subsidence models, see *Galloway and Burbey* [2011]. Concerning 3-D Biot-based software, analyses have recently been carried out by commercial multipurpose finite element simulators such as ANSYS and ABAQUS [e.g., *Hernandez-Marin and Burbey*, 2010, 2012; *Yeh and Sullivan*, 2007]. There are very few exceptions, e.g., the HDM [*Hsieh*, 1996] and GDM [*Burbey and Helm*, 1999] research programs, whose use was limited to simple test cases, and the GEPS3D (Geomechanical Elasto-Plastic 3-D Simulator) code, developed at the University of Padova [*Gambolati et al*., 2001]. In recent years, GEPS3D has been successfully used in several regional-scale geomechanical applications [e.g., *Teatini et al*., 2006; *Ochoa-González et al*., 2013]. An advanced block FSAI-ILU (Factored Sparse Approximate Inverse with Incomplete LU factorization) preconditioner [*Janna et al*., 2012] is implemented into GEPS3D to effectively solve on parallel supercomputers the large linear systems arising from the FE implementation of GEPS3D.

4. Anthropogenic Land Uplift

The simplest, most straightforward action toward mitigating land subsidence caused by fluid withdrawal would seem to be artificial fluid injection. It goes without saying that other strategies can help to prevent land subsidence, including the policy on groundwater pumping exercised by the central and local authorities, requiring withdrawal limits, permits, fees, taxes, metering, and enforcement control. *Freeze* [2000] conveys the general recommendation that land subsidence should act as a guiding factor when defining a

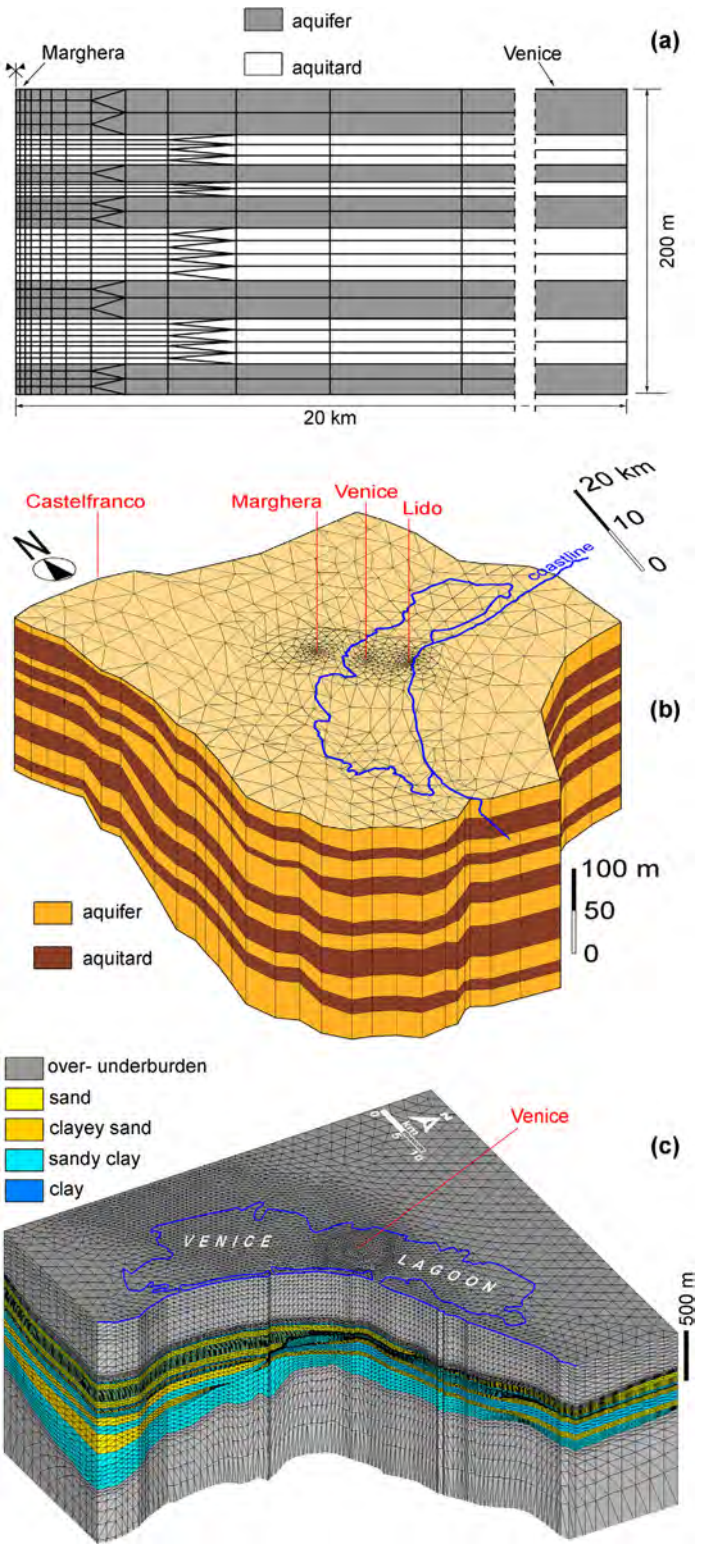

Figure 6. Forty year evolution of FE models used to simulate the geomechanics of the aquifer systems underlying the Venice Lagoon, Italy. (a) Vertical cross section of the 3-D axi-symmetric mesh of *Gambolati et al.* [1974] made from 812 nodes and ≃1000 annular elements (each rectangle was divided into two triangles). The model run on a IBM PS44 (256 Kb RAM). (b) Perspective view of the quasi 3-D mesh of the Venetian multiaquifer system of *Teatini et al.* [1995]. Each aquifer was discretized into 1158 triangles with 608 nodes and each aquitard column into six linear elements, for an overall number of 18,848 nodes. The model run on an IBM RISC6000/560 (512 MB RAM). (c) Axonometric view of the tetrahedral mesh used to predict the anthropogenic uplift of Venice by seawater injection into saline aquifers [*Teatini et al.*, 2011a]. The mesh totaled 1,905,058 elements and 328,215 nodes with simulations performed on a Core-I7, 2.66 GHz processor-based workstation (6 GB RAM).

groundwater exploitation management strategy, along with more traditional factors, such as water table decline, saltwater intrusion, and avoidance of groundwater contamination.

Generally speaking, when land subsidence has occurred and/or is still occurring, methods used to control, mitigate, or arrest it include reduction of pumping rates, artificial aquifer recharge from the land surface, repressurization of depleted layers by way of wells, creation of a hydraulic barrier to stop advancement of the depression cone, and generation of an overpressure in geological units unaffected by pumping in order to build a structural obstacle to the migration of in-depth compaction to the ground surface. A combination of any of the above methods can be used as well, consistent with a cost/benefit analysis. An example of conservative mitigation strategy is one whereby the effective stress within the depleted formation does not increase beyond the stress level experienced to date. A more aggressive strategy might dictate a decrease in the effective stress and/or the active involvement of overlying formations through the use of fluid injection. Injecting water into a geological formation generates an increase in pore pressure, a decrease in effective stress, and hence an expansion of the injected formation. Part of the latter may migrate to the ground surface, giving rise to an anthropogenic land rebound and/or uplift.

While anthropogenic land subsidence is a well-known process, the reverse, namely artificial land uplift, is a much less observed and recognized event, even though the practice of injecting fluids underground is more than a half a century old. Injection technology has been advancing continuously since it came into wide use in the 1950s and 1960s in order to reinject the formation water extracted along with hydrocarbons, or to dispose of industrial wastes. The number of injection wells has grown exponentially, to the point that EPA (the U.S. Environmental Protection Agency) has identified around 400,000 injection boreholes in the USA alone [*USEPA*, 2002]. The injection of water-based solutions, hydrocarbons, CO_2 or N_2 to enhance oil production (EOR) started in the 1940s and soon became an accepted technique for recovering additional oil from reservoirs that were already depleted or water flooded. Thermal recovery processes by vapor injection, used in reservoirs containing heavy (viscous) oil or bitumen, are generally accompanied by an important uplift locally recorded up to 30 cm: examples include the Cold Lake [*Stancliffe and van der Kooij*, 2001], Shell Peace River [*Du et al*., 2008], and Athabasca oil sands [*Collins*, 2007], in Canada.

In the Krechba gas field, Algeria, land rebound was caused by the reinjection of CO_2 separated from the produced gas [*Vasco et al*., 2010]. Storing gas underground may generate a measurable land uplift as well [*Teatini et al*., 2011c]. The aquifer systems underlying Tokyo and Osaka, Japan [*Sreng et al*., 2011] and Taipei, Northern Taiwan [*Chen et al*., 2007], experienced a natural flow field recovery after cutting the water pumpage, and significant land rebound as well.

There are also examples of water being pumped into an oil field to mitigate land subsidence caused by oil production, including the case of Long Beach, California. Here the mitigation program was carefully controlled and monitored [*Pierce*, 1970; *Rintoul*, 1981; *Colazas and Strehle*, 1995]. Water injection started on a major scale in 1958 using appropriately treated seawater collected from shallow wells 30–120 m deep, later mixed with formation wastewaters produced with the oil. Eleven years later, when 2 m^3/s was being pumped into the oil field, the settling area had been reduced from 58 to 8 km^2, with local land surface rebound equal to 30 cm.

Land motion related to subsurface fluid injection went unnoticed for a long time in the vast majority of cases. There are a number of reasons for this. First, in most cases, the disposal of fluids occurred in deserted or sparsely inhabited areas where measuring surface displacements was not a priority, in part due to the large cost of leveling surveys. In other instances, uplift was so slight that no environmental hazards were created and no monitoring program was really needed, or else the area involved was quite limited, with no damage to engineered structures or infrastructures reported or even expected. Only in recent times has satellite technology offered a relatively inexpensive, spatially distributed, accurate methodology for detecting ground movements practically worldwide. It has revealed anthropogenic uplifts of some interest in terms of magnitude, size of the area involved, and time of occurrence. The use of SAR-based techniques has grown rapidly over the last decade, immensely facilitating the detection and measurement of rising areas. This is particularly true for surface movements connected with natural fluctuations of the groundwater head and in areas of aquifer storage (ASR), which have been systematically monitored by the USGS (United States Geological Survey): among others see Santa Clara Valley, California [*Schmidt and Burgmann*, 2003], Santa Ana basin, California [*Galloway and Hoffmann*, 2007], and Las Vegas Valley, Nevada [*Hoffmann et al*., 2001;

Bell et al., 2008]. Measured uplift amounted to 4 cm from 1992 to 1999 in Santa Clara Valley and 3 cm from 2003 to 2005 in Las Vegas Valley. In addition, surface and borehole tiltmeters have been widely used in recent years to monitor ground heave within relatively small areas [*Du et al*., 2008]. For a recent thorough review of areas uplifted anthropogenically by injecting fluid underground see *Teatini et al*. [2011b].

As far as soil compressibility is concerned, the value of α in the first loading cycle is to be used if the aquifer is withdrawn, and in unloading/reloading when the aquifer is recharged/repressurized. The ratio $\alpha_{loading}/\alpha_{unloading}$ decreases with depth and may approach 1 order of magnitude for very shallow silty/clayey sediments [*Teatini et al*., 2011b].

Venice, Italy, is a special case of land uplift predicted with the aid of a finite element (FE) model. An upheaval of the city induced by seawater injection into deep saline aquifers could significantly reduce the frequency of the high tides that periodically flood Venice. Early numerical studies based on a simplified lithostratigraphy of the Venetian subsurface [*Comerlati et al*., 2004] suggested that the city might be raised by pumping seawater into deep aquifers through 12 wells located on a 10 km diameter circle. Using a more accurate 3-D reconstruction of the Quaternary deposits, developed very recently from about 1050 km of multichannel seismic profiles and eight exploration wells, along with a more accurate representation of the injection boreholes, new FE predictions are performed [*Teatini et al*., 2011a] (Figure 6c). The new model simulates the lithostratigraphy of the lagoon subsurface and allows for a reliable assessment of the water volumes injected into the geologic formations based on the actual bottomhole overpressure, which may vary both in space and time. Selection of the best hydraulic conductivity is discussed by *Teatini et al*. [2010], while special consideration should be made for the rock compressibility. In inelastic virgin loading (I cycle) conditions α is provided in Figure 5. However, injection involves unloading the sediments (II cycle). In agreement with *Comerlati et al*. [2004] and *Castelletto et al*. [2008], we have decreased the virgin α of Figure 5 by a factor 3.5. This is also well supported by the most recent findings of *Ferronato et al*. [2013]. Pumping is planned along two Pleistocene sequences originating from the Alps and Apennines sedimentation and terminating just south and north of Venice, respectively, and the shelf portion of a rather continuous Pliocene sequence below the central lagoon, with arenite layers as deep as 1000 m below mean sea level. With a proper tuning of the injection pressure, the model [*Teatini et al*., 2011a] allows for prediction of a fairly uniform 25–30 cm uplift over 10 years after the inception of injection (Figure 2b). The gradient of the predicted vertical displacement ξ_z does not exceed 5×10^{-5} and 1×10^{-5} in the whole lagoon and Venice, respectively, which is well below the most conservative safety limits recommended for masonry structures, even in the presence of a heterogeneous injection aquifer *Teatini et al*. [2010]. If ad hoc calibrated injection overpressure is implemented in each single well, ξ_z may be reduced to as little as 0.1×10^{-5} throughout the city [*Gambolati et al*., 2009].

A pilot experiment has been designed to verify the feasibility of the project for uplifting Venice [*Castelletto et al*., 2008]. The pilot experiment plan foresees three boreholes located at the vertices of a triangle with sides 1 km long, in a lagoon area to be selected (suitable sites might be Cascina Giare, Fusina, Le Vignole, and San Giuliano, all lying in the vicinity of Venices historical center). The aim would be (1) to obtain further detailed lithostratigraphies capable of enhancing our knowledge of the underground lagoon; (2) to perform an injection test with (treated) seawater and measure the overpressure generated in the injected formation; (3) to monitor continuously and in real time the actual land uplift in the area, with the aid of high-precision leveling, GPS, and satellite interferometry; and (4) to set up and experiment with a procedure of optimal control; for instance, the uniformity of uplift may be checked with the aid of sensor feedback automatically accommodating the injection rate in each single well.

For a detailed description of the project of anthropogenic uplift of Venice, its major environmental impact, and expected cost, see *Gambolati and Teatini* [2014].

5. Geomechanical Processes to be Addressed in Future Research

Apart from compaction or expansion, pore pressure change in the withdrawn or injected formation may induce other geomechanical processes, e.g., the generation of local fractures that may extend to the ground surface, reactivation of preexisting faults, with a sharp increase in hydraulic conductivity, and significant reduction of mechanical properties. The consequences may greatly affect ground structures and infrastructures and expose aquifers to the risk of contamination.

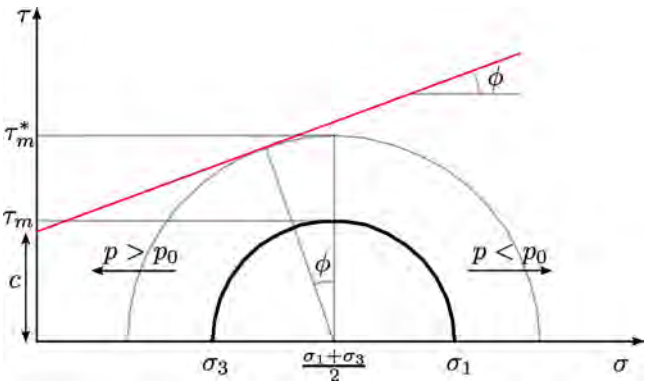

Figure 7. Mohr-Coulomb's circles. When the pore pressure p increases because of fluid injection, the circles move leftward and may achieve the limiting yield surface or friction line $\tau = c + \sigma\tan\phi$ where σ and τ are the normal and shear stress, respectively, c is the cohesion and ϕ is the friction angle. τ_m and τ_m^* are the current largest and maximum allowable shear stress, respectively, σ_1 and σ_3 are the maximum and minimum principal stress, respectively.

These mechanisms are better described with the aid of the Mohr-Coulomb representation of the effective stress state in the (σ, τ)-plane as shown in Figure 7, where compressive stresses are marked as positive. When water is removed, the pore pressure p decreases with respect to the original value ($p < p_0$) and the effective stress σ increases in accordance with Terzaghi's principle. Hence, Mohr-Coulombs circle moves rightward, i.e., farther from the shear-τ-axis and generally, from the failure line bounding the envelope of the allowable stress states. By contrast, when fluid is injected p rises and may exceed p_0. In this case, the effective stress falls below the original in situ value, with Mohr-Coulombs circle moving leftward, i.e., toward the τ-axis and generally, the failure line. It is worth pointing out that during both pumping and injection, the maximum (σ_1) and minimum (σ_3) effective stresses may follow different paths, possibly creating an increase in the diameter of Mohr-Coulombs circle that approaches the failure line (Figure 7) [*Zoback*, 2007]. Two failure mechanisms may occur: (a) if Mohr-Coulombs circle touches the envelope line a shear failure may ensue or a preexisting fault/thrust may be activated, and (b) if Mohr-Coulombs circle crosses the τ-axis a tensile failure takes place. Moreover, a dilation (or dilatancy) phenomenon may be induced, i.e., an increase in volumetric strain due to shear, increasing the magnitude of the injected formations expansion. Shear dilation accompanies yield and strain weakening with permanent alteration in the fabric of the fluid-bearing stratum through irreversible deformation, grain rearrangement, permeability change, and porosity increase, potentially contributing to a measurable rebound of the land surface [*Zoback*, 2007].

We need additional research and development in order to improve our understanding of these processes as they relate to groundwater use. Shifting to discontinuous mechanics from the classical continuum approach traditionally relied upon to investigate land subsidence and uplift, is still a challenging task, at least for large-scale geomechanical occurrences. Major research areas within this framework presently include the prediction of (i) earth fissure formation and shallow fault activation, generally termed as "ground ruptures," and (ii) induced or triggered seismicity. Below we present a brief review on the state of the art concerning such issues.

5.1. Ground Ruptures

Ground ruptures associated with land subsidence caused by groundwater withdrawal have been reported from many alluvial basins in semiarid and arid regions since the late 1970s. Likely examples are recorded in the southwestern USA [*Holzer et al*., 1979; *Jachens and Holzer*, 1982; *Holzer and Galloway*, 2005], central Mexico [*Pacheco et al*., 2006; *Carreón-Freyre et al*., 2010, 2011], Iran [*Ziaie et al*., 2009; *Mahmoudpour et al*., 2013], Saudi Arabia [*Bankher and Al-Harthia*, 1999], and China [*Li et al*., 2000; *Shi et al*., 2007; *Wang et al*., 2009].

Fissure development has been observed both within areas where natural resources are exploited and along the areas boundaries. Density, shape, length, aperture, depth, and dislocation of the fissures vary greatly from site to site, and are mainly related to subsoil lithostratigraphic variations. In several places only a few isolated fissures have formed; in others, many. More than 2 m vertically dislocated fissures have been observed, up to 15 km long, 1–2 m wide, and 15–20 m deep. Considerable economic, social, and environmental damage is reported: rupture of borehole casings, pipes, and canals used for withdrawing groundwater and conveying water, oil and gas, with negative consequences both in rural zones, where the water is mainly used for crop production (e.g., in the Sarir agricultural area, Libyan desert, and in southcentral Arizona), and in urban areas (e.g., in Mexico City, Quertaro, and Celaya located within the Transmexican Volcanic Belt in Mexico; in Beijing, Xian, Wuxi in China). Other consequences include: reduction of potable

Figure 8. Picture showing consequences of land subsidence and ground ruptures due to groundwater overdraft. (a) Riva degli Schiavoni at Venice flooded during the high tide recorded on 12 February 2013. (b) Protrusion of a wellbore located in the eastern part of Mexico City where land subsided by approximately 8 m between 1936 and 2013. WP: well pump and WC: well casing [after *Hernández-Espriú et al*., 2014]. (c) The 13 m deep Rodgers earth fissure occurred in September 1997 in Maricopa County, Arizona (courtesy of The Arizona Geological Survey, photo by Joe Cook shot in November 2008). (d) Street crack and structural damage to buildings in the city of Xian, China, as of 2014 (courtesy of Shujun Ye, Nanjing University, China).

water supply; cost increase in groundwater extraction; damage to surface structures (e.g., houses, historical palaces, churches, and other buildings); cracking of infrastructures such as streets, water pipes, railways, and runways; injuries to livestock and other animals as well as to people; creation of preferential flow paths for contaminants from the surface into shallow aquifers; and triggering of severe soil erosion and creation of badlands topography near the rupture (Figure 8).

Several mechanisms have been proposed to explain the origin of ground rupture associated with the development of natural resources, see Figure 9a for a representation of few of them [*Holzer et al*., 1979; *Sheng*

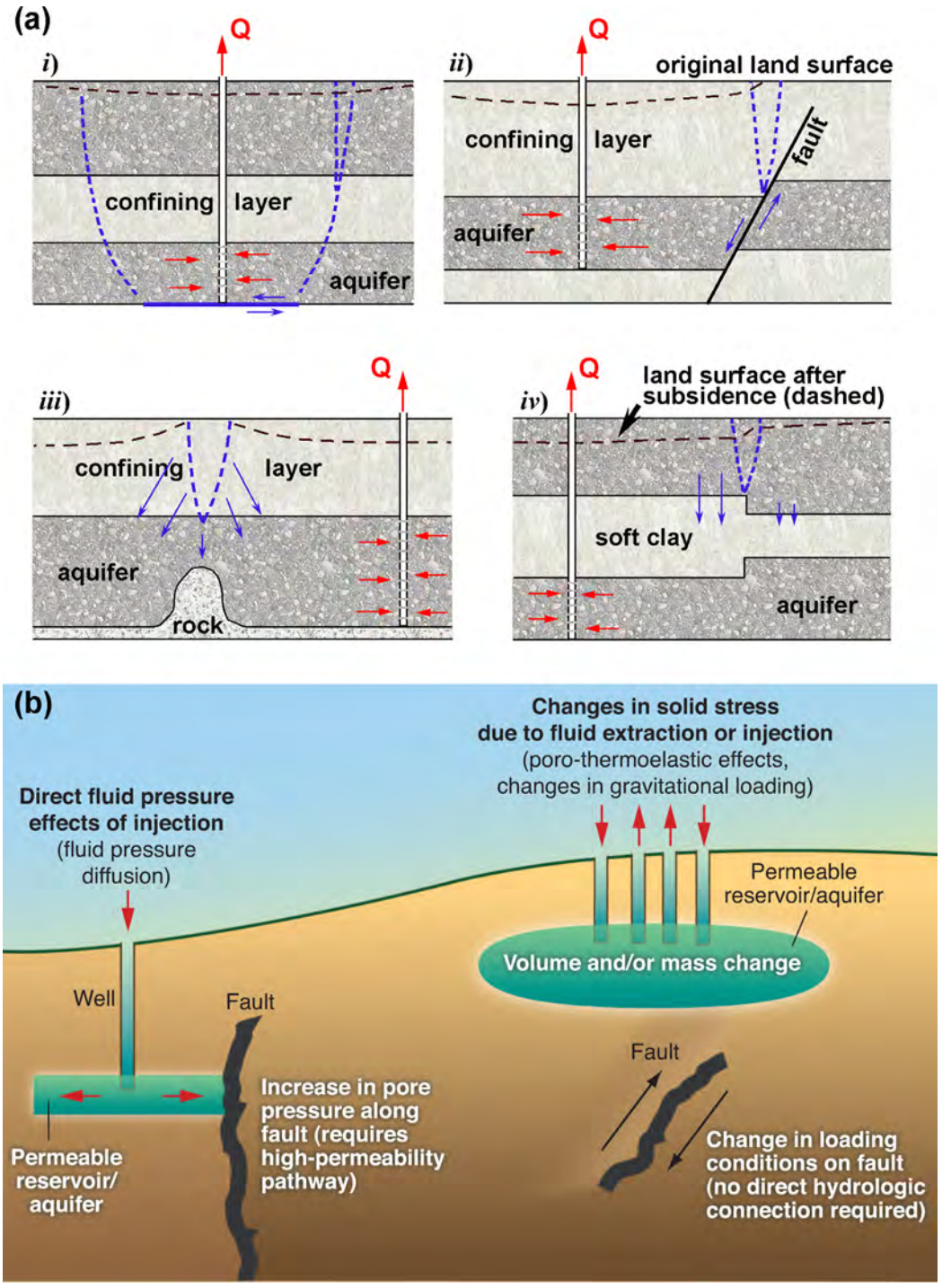

Figure 9. (a) Sketch of the mechanisms inducing ground ruptures: (i) horizontal displacement due to shearing on the plane of weakness or to tensile failure; (ii) reactivation of an existing fault caused by horizontal displacements; (iii) tensile fracture above a bedrock ridge; (iv) differential compaction due to heterogeneous thickness of aquifer (rigid)/aquitard (compressible) layers (modified after *Sheng and Helm* [1998]). (b) Sketch of the mechanisms inducing earthquakes: (left) pore pressure increase or (right) change of the geostatic load in the vicinity of a fault. In the above cases, both the effective normal and tangential stresses acting on the fault change, causing fault reactivation [after *Ellsworth*, 2013].

and Helm, 1998; *Sheng et al.*, 2003]. According to the direction of pumping-induced stresses below the surface, we may identify two main types of ground rupture: tensile fissures and shear fissures [*Holzer and Pampeyan*, 1981]. The main difference between these two fissure types is the vertical offset observed in the field. Typically, tensile-induced earth fissures create slight or no offsets, while shear-induced earth failures

emerge in the field as having measurable scarps [*Holzer and Pampeyan*, 1981]. However, this distinction may be very difficult to recognize in urban areas, where some shear-induced ruptures initially appear without any vertical offset, as structures/infrastructures on the land surface mask the actual rupture displacements.

Starting from the early 2000s, research was mainly focused on modeling, and hence predicting, ground failure. A Mohr-Coulomb failure criterion was used by *Budhu* [2008] to analyze fissure initiation in heterogeneous sedimentary deposits. He found that the most potent mechanism for earth fissures formation combines bending and shearing. Geological discontinuities are the preferred location for ground failure to occur, with ruptures that initially form at the surface and then propagate downward, or vice versa, depending on the prevailing mechanisms. Using a continuum approach and the ABAQUS elastoplastic geomechanical simulator, *Hernandez-Marin and Burbey* [2010, 2012] studied the spatial distribution of deformation, and normal and shear stresses that potentially lead to the formation of ground ruptures. Their results indicate that the presence of a preexisting fault zone largely controls the deformation and stress regime of the porous medium during pumping, with areas of stress accumulation that may eventually lead to fissure formation. The simulations were carried out on 2-D vertical sections representing the Las Vegas Valley.

Recently, an original numerical approach based on "Interface Elements" (IE), developed to simulate the possible activation of regional faults due to hydrocarbon production [*Ferronato et al.*, 2008; *Jha and Juanes*, 2014], has been used to carry out preliminary simulations of earth fissure generation and propagation caused by groundwater pumping [*Janna et al.*, 2010]. The geomechanical model is based on the structural equations of poroelasticity solved in a three-dimensional setting with the aid of the FE-IE approach. While standard FEs are used to represent a continuum, IEs prove especially effective in examining the relative displacements of adjacent elements, such as the opening and slippage of preexisting faults or the generation of new fractures, by using an elastoplastic constitutive law based on the Mohr-Coulomb failure criterion. A zero-thickness IE compatible with linear FE consists of a pair of linear elements (1-D in a 2-D problem, 2-D in a 3-D problem) with the opposite nodes coinciding. The interface displacements in the local reference frame associated with each element are the aperture δ_n and the slippage δ_{s1} and δ_{s2} between the "top" and the "bottom" face of the element. The displacement components are related to the interface stresses σ_n, τ_{s1}, and τ_{s2}, with σ_n taken as the normal stress (negative in compression, positive in expansion), and τ_{s1} and τ_{s2} as the shear stress components in the interface plane. Irreversible plastic displacements of the interface may take place wherever the limiting tensile or the shear strength are exceeded. Assuming conservatively that no tensile strength is allowed, the opening of fissure/fault surfaces occurs when the stress normal to the interface plane, i.e., σ_n, becomes positive. Irreversible slip occurs when the Mohr-Coulomb failure criterion is violated. Sealing fissures, i.e., ones with a no-flux surface, are simulated allowing the pressure gradient acting on the contact surface to be different.

5.2. Induced Seismicity

In recent years, concerns have been raised about the risk of inducing or triggering a seismic activity as a consequence of pumping water from or injecting it into geologic formations [*Ellsworth*, 2013].

Very recently, injection-induced earthquakes have become a discussion topic and a focus for research in connection with (i) hydraulic fracturing of tight shale formations for hydrocarbon production; (ii) disposal of wastewaters; and (iii) enhanced geothermal systems. The activation of thrusts/faults caused by groundwater withdrawal (as well as by fluid injection) may pose a very serious hazard of anthropogenic seismicity. According to *Ellsworth* [2013], the mechanism responsible for inducing seismicity "appears to be the well-understood process of weakening a pre-existing fault" by changing the fault loading conditions. In essence, "increasing the shear stress, reducing the normal stress and/or elevating the pore pressure can bring the fault to failure triggering the nucleation of an earthquake" (Figure 9b). The number of earthquakes with magnitude $M \geq 3$ recorded yearly in the USA midcontinent has grown significantly since 2001, with anthropogenic earthquakes suspected as being largely responsible for the increase (Figure 10). Earthquake initiation and propagation is site-dependent, influenced by fault frictional properties and geometry, the preseismic natural stress regime, stress changes induced by anthropogenic activity, and the volume of injected or pumped fluid.

Several cases have been reported in which microseismic events were correlated directly to fracking. These cases are notable because of the public concern they raised, although the magnitude was too slight to create

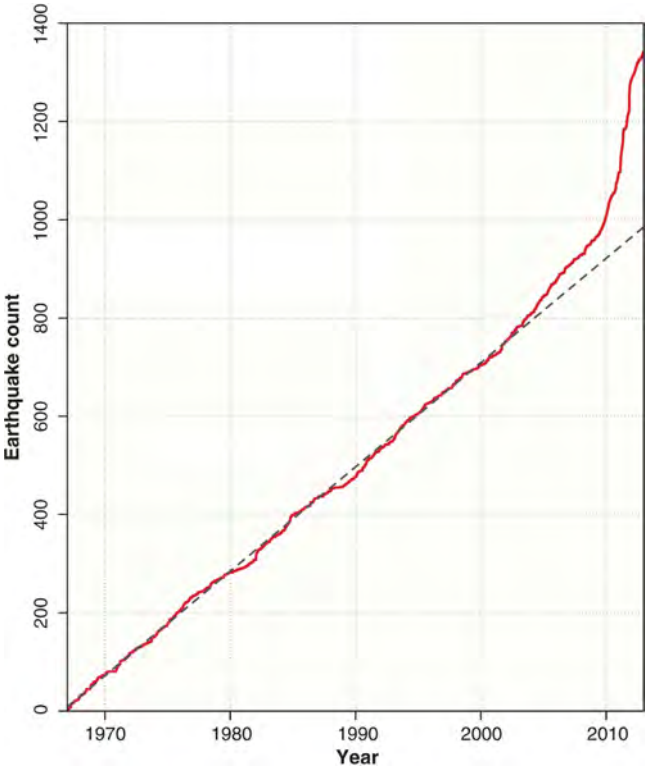

Figure 10. Number of earthquakes with magnitude $M>3$ recorded in the mid-U.S. from 1967 to 2012 [after *Ellsworth*, 2013].

appreciable damages. Extracting hydrocarbons from shale requires the generation of a network of open fractures connected to the producing boreholes. This is accomplished by way of a high-pressure injection of water into the formation. Thus, fracking intentionally induces numerous microseismic events, the vast majority of which with $M < 1$. However, a number of cases have recently been experienced where earthquakes large enough to be felt correlated directly to hydraulic fracturing. *Holland* [2013] investigated a sequence of events in south-central Oklahoma, with maximum $M = 2.9$, revealing a clear temporal correlation between fracking operations in a nearby well and seismic activity. On April 2011, the Blackpool area of northern England experienced seismicity of magnitude 2.3 shortly after the hydraulic fracturation of a well to develop a shale gas reservoir in the Bowland basin [*The Royal Society and the Royal Academy of Engineering*, 2012].

Injection disposal wells appear to have triggered or induced several earthquake sequences in the midwestern U.S. Before 2011, the $M = 4.8$ event in 1967 near Denver, Colorado, was the largest event widely accepted in the scientific community as having been induced by wastewater injection [*Hermann and Park*, 1981]. By that time, the earthquakes had migrated as far as 10 km from the injection point along an ancient fault system, tracing a critical pressure front of 3.2 MPa. Wastewater disposal appears to have induced over 109 small earthquakes ($0.4 < M < 3.9$) from January 2011 to February 2012 in Youngstown, Ohio, close to a deep fluid injection well. The main shocks occurred at depths between 3500 and 4000 m along a fault located in the Precambrian basement [*Kim*, 2013]. A similar situation was observed in central Arkansas [*Horton*, 2012].

A number of studies have explored the response of water injection-induced activity in enhanced geothermal systems. The most prominent example is an $M = 3.4$ event induced in 2006 by the stimulation of a geothermal reservoir below the city of Basel, Switzerland, at a depth of about 5000 m [*Häring et al.*, 2008]. Thousands of smaller shocks were recorded afterward, leading insurance companies to claim over 7 million euros in damage. In 2003, at the geothermal site of Soultz-sous-Forts, France, stimulation of the $\simeq$4800 m deep reservoir produced seismic events with magnitude of up to $M = 2.9$ in 2003 [*Baisch et al.*, 2010]. Epicenters align along a preexisting subvertical regional-scale fault structure. A hot-fractured-rock project was launched at Cooper Basin, South Australia, in 2002 to exploit the Habanero granite reservoir at a depth of 4000–4500 m. Various stimulation experiments have been conducted which triggered earthquakes with moment magnitude between 1.7 and 3.1 with hypocentral distances between 2.4 and 7.8 km and depth between 3900 and 4500 m [*Baisch et al.*, 2006]. In these cases, thermal drawdown of the rock superpose to the pressure change due to fluid injection causing significant changes in the effective stress regime, which in turn can increase the likelihood of fault reactivation and consequently, induced seismicity [*Gan and Elsworth*, 2014].

As regards the possibility of inducing seismic events by groundwater pumping, the $M = 5.1$ earthquake that occurred in May 2011 in Lorca, southeast Spain, is a renowned case study. The earthquake struck the city of Lorca causing significant property damage, injuring hundreds of people and resulting in nine casualties.

The hypocenter was located in a complex, active system of strike-slip faults at a depth of 3 km. According to *González et al*. [2012], the event may have been triggered by the significant crustal unloading caused by the ≃250 m drop in groundwater level occurring between 1960 and 2010 as a consequence of aquifer overdraft. The decrease in total stress may have relaxed the effective normal stress acting on the fault plane, thus triggering its reactivation. However, we should note that there exists no general consensus as regards the relation between piezometric lowering and the 2011 event.

A reconnaissance study aiming to identify major geological discontinuities is of paramount importance, along with a modeling tool capable of predicting fault/thrust activation resulting from the removal or injection of fluid [*Ferronato et al*., 2008; *Gan and Elsworth*, 2014; *Jha and Juanes*, 2014; *Teatini et al*., 2014]. With the aid of an ad hoc model we can estimate the sliding of the fault/thrust, and hence predict the seismic moment.

The seismic literature presents several empirical relationships enabling us to predict the possible magnitude M induced by a fault/thrust reactivation. Recently, *Mazzoldi et al*. [2012] have suggested an equation based on the seismicity theory that provides an estimate of the seismic moment M_0 of a possible seismic event induced or triggered by a fault/thrust slip:

$$M_0 = G \cdot \Delta L \cdot \Delta Z_a \cdot s_a \tag{22}$$

where ΔL and ΔZ_a are the horizontal length and height, respectively, of the activated portion of the fault/thrust, s_a the average slip of the fault/thrust surfaces and the $G = 0.5\vartheta E_v/(1-\nu_h)$, with $E_v = [1-2\nu_v^2/(1-\nu_h)/\vartheta]/\alpha$ [*Janna et al*., 2012], is the shear modulus of the formation incorporating the reactivated fault/thrust. The seismic moment M_0 obtained from equation (22) may be converted into a moment magnitude M used to measure the strength of the seismic event. The M_0-M relationship is defined as follows [*Kanamori and Anderson*, 1975]:

$$M = \frac{2}{3}(\log_{10} M_0 - 9.1) \tag{23}$$

with M_0 expressed in (Nm). As far as G is concerned, we have to use the value of α in the first loading cycle if the aquifer is withdrawn, and in the second unloading/reloading phase if the aquifer is recharged/repressurized.

6. Measuring Deformation of Aquifer Systems and Land Displacements

The development of appropriate methodologies for measuring the geomechanical effects induced by groundwater withdrawal has been a major issue since the early decades of the past century. Since then, interest has been focused on two interconnected topics: (i) the deformation, i.e., compaction or expansion, of withdrawn aquifers and intervening silty-clayey layers; and (ii) the movement, i.e., land subsidence or uplift and horizontal displacements, of the land surface.

6.1. Deformation Measurements

Continuous measurements of soil deformation in a (normally small) number of locations in a subsiding area have been carried out using borehole extensometers. They are used to measure the change in the distance between the land surface and a subsurface benchmark situated at the bottom of a deep borehole. If the subsurface benchmark is established below the base of the compacting aquifer system or in the bedrock, the extensometer can be used as the stable reference for local geodetic surveys. The first borehole extensometer was installed in 1955 by the U.S. Geological Survey in the San Joaquin Valley, California [*Poland*, 1984]. Since then, extensometer technology has seen progressive improvement, playing an important role in relating land subsidence to the compaction of confined aquifer systems. Several types of early borehole extensometers are reviewed by *Poland* [1984]. Recently, anchored cable counterweighted extensometers and slip-joint casing extensometers have been widely used. The measuring devices are schematically shown in Figures 3a and 3b. A typical cable counterweighted extensometer tool consists of a balance beam carrying a cable or a pipe, which is fastened at one end to an anchor weight located at the bottom of the compacting system, and at the other end to a counterweight keeping the cable at a constant tension (Figure 3a). To build up a sliding-joint casing extensometer, a hole is drilled to a depth where rock is stable. The hole is then lined with a steel casing with slip-joints to prevent crumpling as subsidence occurs. An inner pipe rests on a concrete plug at the bottom of the borehole and extends to the top. This inner pipe then

transfers the stable elevation below to the surface. Measurement of the distance from the inner pipe to the surrounding land surface provides the amount of compaction that has occurred over a given time interval (Figure 3b). A computer-controlled system records the compaction data against time. The instrumental precision heavily depends on the actual extensometer implementation, but a nominal strain resolution of 0.01–0.1 mm can be achieved over a 200–1000 m depth [*Riley*, 1986]. In the case of multiaquifer systems, extensometric stations are composed of close multiple-borehole extensometers installed at different depths, so as to derive the deformation of each single formation by subtracting the records acquired at various depths. A recent alternative to multiple-extensometric stations are multiple-position borehole extensometers that incorporate a number of independent markers anchored to the formation borehole at different depths (Figure 3c). Magnetic markers have been used in Taiwan [*Hwang et al*., 2008; *Hung et al*., 2012] to compute vertical compaction in boreholes using repeat borehole logging with magnetic sensors on calibrated lines or tapes in order to measure temporal changes in marker positions. This method is capable of monitoring from ten to several tens of marker positions in a single borehole at measurement resolutions of about 1–2 mm over a depth of several hundred meters.

A relatively dense network of extensometric stations has been established in metropolitan areas experiencing significant land subsidence. Two major examples are Houston, Texas, and Shanghai, China. The Houston-Galveston area is an extreme example of subsidence hazards, a problem that affects many other U.S. metropolitan areas, e.g., Los Angeles (CA), Sacramento (CA), and New Orleans (LA). Portions of Houston experienced severe settlement, up to 3 m, from 1915 to 2001. The USGS has been operating 13 borehole extensometers at 11 sites since 1973 for the purpose of observing compaction of aquifers in the whole area. The borehole extensometers, which were designed according to the sliding-joint casing type, span a depth down to 936 m [*Yu et al*., 2014]. Shanghai is the first city in China where land subsidence was investigated and monitored, being one of the country's most densely populated and developed areas. The maximum cumulative land subsidence was 2.6 m in 2002 and the total area of land subsidence was about 5000 km^2 in 2006. A number of 27 extensometer groups have been used since the 1960s to monitor compaction of individual aquifers and aquitards to a depth of approximately 350 m [*Wu et al*., 2010].

Horizontal extensometers were used to measure differential horizontal ground motion at earth fissures caused by changes in groundwater levels in South-Central Arizona [*Carpenter*, 1993]. Buried horizontal extensometers made of quartz tubes or Invar wires were used to precisely and continuously measure fissure opening in a natural environment over a scale of 330 m. Following enlargement of the ground rupture occurrence in several countries worldwide, other specific mechanical and optical instrumentation has recently been developed and established in urban areas such as Iztapalapa, Mexico City [*Carreón-Freyre et al*., 2010], and Beijing [Zhu et al., 2015]. These monitoring stations allow one to accurately measure the relative displacements characterizing the rupture in a 1-D (only opening) or 3-D (opening and sliding) reference system (Figure 11).

6.2. Displacements of the Land Surface

A countless number of scientific papers have been published over the last two decades concerning interferometric Synthetic Aperture Radar (SAR)-based methodologies for measuring displacements in the earth surface, in particular, land movements due to groundwater pumping [e.g., *Amelung et al*., 1999; *Hoffmann et al*., 2001; *Buckley et al*., 2003; *Hoffmann et al*., 2003; *Schmidt and Burgmann*, 2003; *Galloway and Hoffmann*, 2007; *Bell et al*., 2008; *Higgins et al*., 2013, 2014]. Differential SAR Interferometry (DInSAR) [*Gabriel et al*., 1989], Permanent Scatterer InSAR (PSInSAR) [*Ferretti et al*., 2001], Small Baseline Subset (SBAS) [*Berardino et al*., 2002], Interferometric Point Target Analysis (IPTA) [*Wegmüller et al*., 2004], and "Squeezed" SAR (SqueeSAR) [*Ferretti et al*., 2011] are only the most well-known and widely used SAR processing-chains among a continuously increasing variety of algorithms. SAR-based techniques exploit the phase difference of the radar signals between or among a number (at least two) of satellite acquisitions over the same area. The phase difference is strictly related to the earth surface displacement occurring between the image acquisitions, once the surface topography contribution is removed and the atmospheric disturbance mitigated. SAR-based methodologies allow for the detection and measurement of subcentimeter-scale ground movement with high spatial detail and high measurement resolution. Several SAR-borne satellites have been in operation from 1991 to the present (ERS-1/2; ENVISAT; JERS-1; Radarsat-1/2, ALOS, TerraSAR-X, Cosmo-SkyMed, and SENTINEL-1 from the mid-2014), thus a large satellite SAR data archive exists over many areas. Figure 12 shows a few significant examples of SAR-derived land subsidence.

Figure 11. Some examples of ad hoc instrumentation developed to monitor opening and sliding of earth fissures or faults activated by the overdraft of aquifer resources. (a) 1-D apparatus and (b) 3-D apparatus established in Iztapalapa, Mexico City (courtesy of Dora Carreón-Freyre, Centro de Geociencias, UNAM, Mexico). (c) 3-D instrumentation installed in the northern Beijing plain (courtesy of Lin Zhu, Normal Capital University, Beijing, China).

As in the case of leveling, SAR-based data are differential measurements, i.e., displacements relative to a reference point. Therefore, the movement of the reference point has to be known, e.g., from previous leveling or permanent GPS stations, in order to calibrate the SAR results and obtain "absolute" displacements. Usually from medium to small-scale investigations (in the order of 10×10 km^2), one reference point suffices for the calibration [e.g., *Brooks et al*., 2007]. Conversely, for large-scale SAR investigations, several reference measurements evenly distributed over the area of interest are required to condition the interferometric outcome [e.g., *Teatini et al*., 2012], since an inaccurate estimate of the orbital baseline results from imperfect knowledge of the satellite position in a phase tilt. The "right solution" in terms of SAR average velocity is possibly rotated on a slightly inclined plane, with the relative displacement rate for radar reflectors some tens of kilometers apart, with an uncertainty of 1–3 mm/yr [*Strozzi et al*., 2001]. To overcome, or at least mitigate, this so-called "flattening" problem, the calibrated SAR solutions must be postprocessed using known displacements provided by leveling and GPS stations. Another typical problem encountered in the calibration of SAR results is the lack of radar targets in the vicinity of the reference point, or the location of such a point on a structure different from those constituting the nearby reflectors. To avoid these inconveniences, which may introduce quite a large degree of uncertainty in the calibration procedure, appropriate stations such as the ones shown in Figure 13, made from one or two artificial radar reflectors anchored together with a GPS antenna, have been successfully tested in the Po River Plain, Italy.

SAR-based measurements are 1-D measurements related to the projection along the satellite Line Of Sight (LOS) of the 3-D displacement vector affecting the radar target. Being the radar viewing angle less than 45°

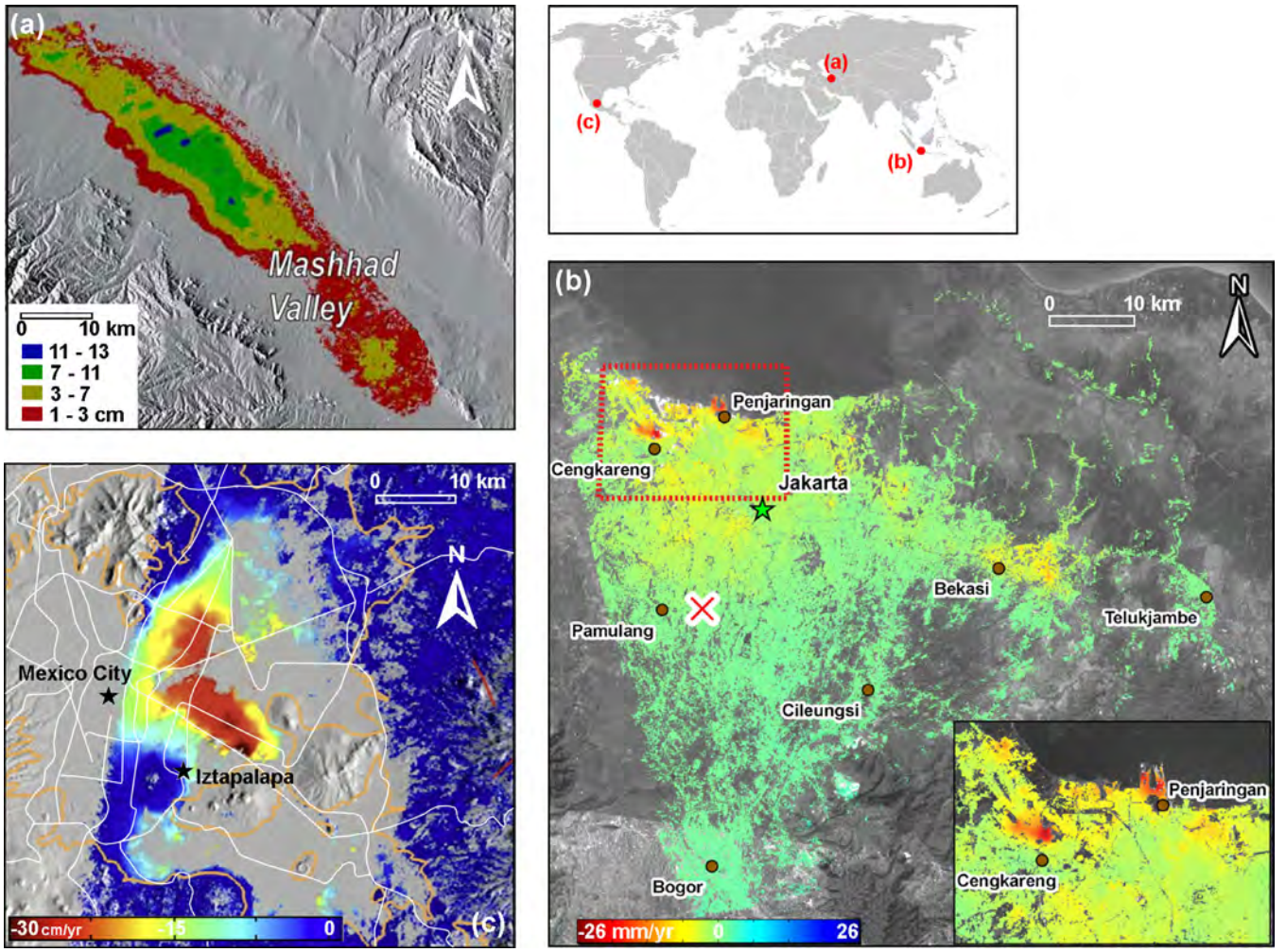

Figure 12. Example of land displacement due to groundwater withdrawal recently detected by SAR-based interferometry. (a) Land subsidence (cm) at Mashhad, Iran, between 14 June 2004, and 1 November 2004; ENVISAT satellite [*Motagh et al*., 2008]. (b) Average subsidence rate in Jakarta, Indonesia, from January 2007 to September 2010; ALOS satellite [*Ng et al*., 2012]. (c) Average 2007–2011 subsidence rate in Mexico City, Mexico; ALOS satellite [*Chaussard et al*., 2014]. Displacements are along the line of sight.

from the vertical, SAR outcome is most sensitive to vertical motion. However, the combination of the Earth's rotation and satellite motion makes it possible for any area of interest to be illuminated by the satellite radar sensor along two different acquisition geometries: one having the satellite flying from south to north (called ascending mode) and the other from north to south (called descending mode). Whenever two data sets of SAR images are available, acquired over the same area and during the same time frame along ascending and descending orbits, the SAR results can be used successfully to estimate two components of the local displacement, i.e., the vertical and the west-east components, thus significantly improving our understanding of the event under study [*Teatini et al*., 2011c]. In the contest of groundwater geomechanics, this approach opens an impressive new perspective in the monitoring of ground ruptures, where horizontal displacements may often be considerable. A noteworthy example is shown in Figure 14.

SAR processing-chains can provide millions of data points over a large region (10^4-10^5 km^2/scene) and are often less expensive than sparse point measurements from "traditional" labor-intensive spirit-leveling and costly GPS stations. Moreover, SAR results have shown that land displacements due to groundwater withdrawal and injection are characterized by a spatial variability almost impossible to detect by other surveying techniques. For these reasons, leveling and GPS have been less and less used over recent years to measure land subsidence. However, we must emphasize that they remain of paramount importance in calibrating the SAR outcome as described above, and are essential in providing measurements over natural terrain,

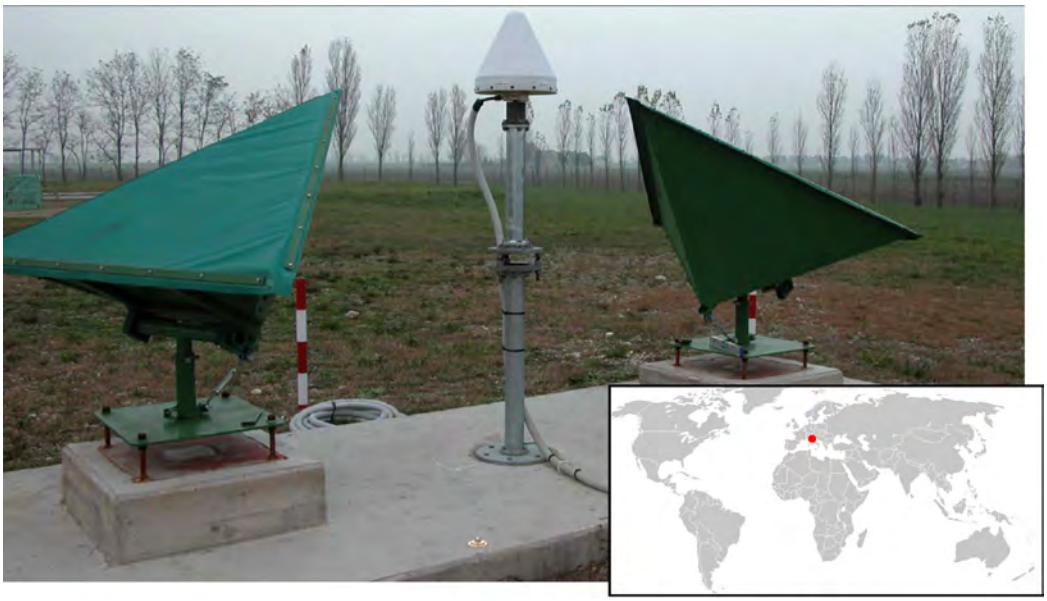

Figure 13. Monitoring station setup from a pair of trihedral corner reflectors, a GPS antenna, and a leveling benchmark established by eni S.p.A. in the Po River Plain, Italy, to provide an accurate reference point for SAR-based investigation.

densely vegetated zones, or farmlands where the SAR signal loses coherence and the interferometric algorithm cannot be applied.

Finally, it is worth mentioning that surface and borehole tiltmeters have recently been used to precisely detect land displacements over a relatively small area. For example, high-resolution borehole tiltmeters installed at five locations at a variable 1.5–3.3 m distance from the injection well denoted as Kontinentale Tiefbohrung der Bundesrepublik Deutschland (KTB) have been extensively used to monitor ground heave due to a water injection experiment performed from June 2004 to April 2005 in the Upper Palatinate, Eastern Bavaria, Germany [*Jahr et al*., 2005].

7. Concluding Remarks

Anthropogenic land subsidence as related to subsurface fluid production has been known for almost a century. Groundwater withdrawal is the primary cause of the occurrence worldwide. Although overall damage is estimated today at billions of dollars a year [e.g., *Borchers and Carpenter*, 2014], with an expected increasing trend due to population and economy growth, the sinking of land is still a problem underevaluated by both governments and public opinion, especially in developing countries. The loss of conveyance capacity in canals, streams and rivers, diminished effectiveness of levees, damage to roads, bridges, buildings, water wells, pipelines, and other surface structures and infrastructures, increasing vulnerability to saltwater intrusion, contamination of shallow aquifers through ground ruptures, and even a greater risk of deaths due to the flooding of coastal and inland urban areas (e.g., New Orleans, Louisiana and Mexico City), are the major consequences of land subsidence. The environmental impact of land subsidence has shifted over the last decade from rural and industrial sites (e.g., the Antelope Valley, California, or the Po River delta, Italy) to urban centers because of the population increase and its concentration in mega-cities. Whereas in 1950, New York was the only urban area totaling more than 10 million people, presently more than 30 cities in the world exceed this impressively large number, most of them located on coastland of developing countries.

The mechanisms underlying the basic process are well understood and universally accepted, and the mathematical modeling of past events and expected future evolution is well established. Modern computer technology allows for the simulation of complex geology and geometry in subsiding basins, of arbitrarily distributed pumping rates, of heterogeneity, anisotropy and nonlinearity of the porous media properties, with a degree of accuracy inconceivable until only a few years ago. Measuring and monitoring

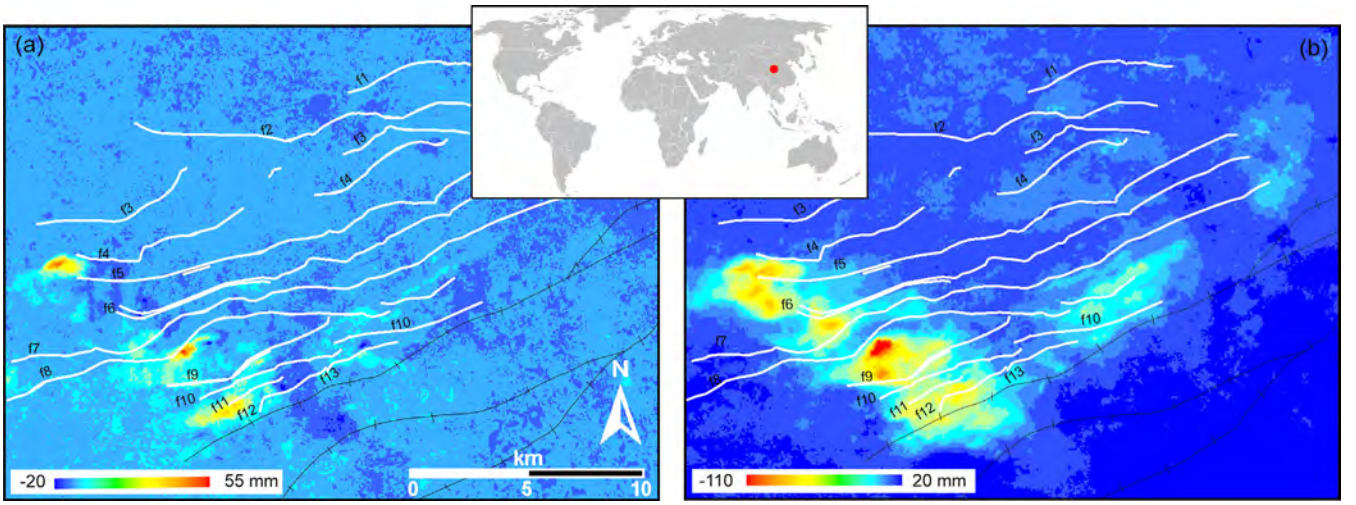

Figure 14. (a) West-east and (b) vertical displacements (mm) in 2009 at Xi'an, China, obtained by simultaneously processing ALOS descending and TerraSAR-X ascending images (modified after *Qu et al*. [2014]).

anthropogenic land subsidence is presently at a very advanced stage, especially with the aid of satellite technology. Scientists can help support decision makers toward predicting, preventing or at least mitigating land subsidence successfully, although certain specific areas may still require more in-depth investigation. These include the 3-D deformation and stress fields correlating to groundwater pumping, uplift caused by water injection, and inverse modeling calibration. Land subsidence rates have been drastically reduced in several places around the world, e.g., Venice, Tokyo, and more recently Shanghai, by exploiting water resources different from groundwater. However, for the majority of other mega-cities or large cities, this target is not within easy reach. This is why land subsidence was recently mentioned as one of the most urgent threats to sustainable development, in the latest UNESCO International Hydrological Program VIII (2014–2020).

Major research advancements must still be accomplished in the face of other geomechanical processes, including earth fissuring, hydraulic fracturing, fault activation, and induced seismicity, which may result from a considerable drop in pore pressure, or from subsurface water injection where injection pressure exceeds the preexisting natural value. These processes require approaches developed in the field of discontinuous mechanics, approaches only partially assimilated in geosciences so far. Significant progress has been made in understanding such process' theoretical mechanisms. However, monitoring their occurrence, characterizing their rheological properties, and developing reliable, robust, and accurate numerical models still pose major challenges for research efforts in the near future.

Acknowledgments
The authors are grateful to the Editor in Chief Alberto Montanari for inviting them to contribute a paper on geomechanics of groundwater subsurface flow to celebrate the 50th WRR anniversary. The data for this paper are available by contacting the corresponding author.

References

Aichi, M. (2008), Coupled groundwater flow/deformation modelling for predicting land subsidence, in *Groundwater Management in Asian Cities: Technology and Policy for Sustainability*, edited by S. Takizawa, pp. 105–124, Springer, Tokyo.

Allen, S. A. (1984), Types of land subsidence, in *Guidebook to Studies of Land Subsidence Due to Ground-Water Withdrawal*, edited by J. F. Poland, pp. 291–305, UNESCO, Paris.

Allis, R., C. Bromley, and S. Currie (2009), Update on subsidence at the Wairakei-Tauhara geothermal system, New Zealand, *Geothermics*, *38*, 169–180.

Amelung, F., D. Galloway, J. W. Bell, H. A. Zebker, and R. J. Laczniak (1999), Sensing the ups and downs of Las Vegas: InSAR reveals structural control of land subsidence and aquifer system deformation, *Geology*, *27*, 483–486.

Aobpaet, A., M. C. Cuenca, A. Hooper, and I. Trisirisatayawong (2013), InSAR time-series analysis of land subsidence in Bangkok, Thailand, *Int. J. Remote Sens.*, *34*(8), 2969–2982.

Baisch, S., R. Weidelr, R. Vörös, D. Wyborn, and L. De Graaf (2006), Induced seismicity during the stimulation of a geothermal HRF reservoir in the Cooper Basin (Australia), *Bull. Seismol. Soc. Am.*, *96*(6), 2242–2254.

Baisch, S., R. Vörös, E. Rother, H. Stang, R. Jung, and R. Schellschmidt (2010), A numerical model for fluid injection induced seismicity at Soultz-sous-Forêts, *Int. J. Rock Mech. Min. Sci.*, *47*, 405–413.

Bankher, K. A., and A. A. Al-Harthia (1999), Earth fissuring and land subsidence in Western Saudi Arabia, *Nat. Hazards*, *20*, 21–42.

Baú, D., M. Ferronato, G. Gambolati, and P. Teatini (2002), Basin-scale compressibility of the Northern Adriatic by the radioactive marker technique, *Géotechnique*, *52*(8), 605–616.

Bawden, G. W., W. Thatcher, R. S. Stein, K. W. Hudnut, and G. Peltzer (2001), Tectonic contraction across Los Angeles after removal of groundwater pumping effects, *Nature*, *412*, 812–815.

Bear, J. (1972), *Dynamics of Fluids in Porous Media*, Elsevier, N. Y.
Bear, J., and M. Y. Corapcioglu (1981a), Mathematical model for regional land subsidence due to pumping: 1. Integrated aquifer subsidence equations based on vertical displacement only, *Water Resour. Res.*, *17*(4), 937–946.
Bear, J., and M. Y. Corapcioglu (1981b), Mathematical model for regional land subsidence due to pumping: 2. Integrated aquifer subsidence equations for vertical and horizontal displacements, *Water Resour. Res.*, *17*(4), 947–958.
Bell, J. W., F. Amelung, A. Ferretti, M. Bianchi, and F. Novali (2008), Permanent scatterer InSAR reveals seasonal and long-term aquifer system response to groundwater pumping and artificial recharge, *Water Resour. Res.*, *44*, W02407, doi:10.1029/2007WR006152.
Berardino, P., G. Fornaro, R. Lanari, and E. Sansosti (2002), A new algorithm for surface deformation monitoring based on small baseline differential SAR interferograms, *IEEE Trans. Geosci. Remote Sens.*, *40*(11), 2375–2383.
Biot, M. A. (1941), A general theory of three-dimensional consolidation, *J. Appl. Phys.*, *12*(2), 155–164.
Biot, M. A. (1955), Theory of elasticity and consolidation for a porous anisotropic solid, *J. Appl. Phys.*, *26*(2), 182–185.
Borchers, J. W., and M. Carpenter (2014), *Land subsidence from groundwater use in California*, Full Report of Findings, report, California Water Foundation, 151 pp.
Bouwer, H. (1977), Land subsidence and cracking due to groundwater depletion, *Ground Water*, *15*(5), 358–364.
Brooks, B. A., M. A. Merrifield, J. Foster, C. L. Werner, F. Gomez, M. Bevis, and S. Gill (2007), Space geodetic determination of spatial variability in relative sea level change, Los Angeles basin, *Geophys. Res. Lett.*, *34*, L01611, doi:10.1029/2006GL028171.
Buckley, S. M., P. A. Rosen, S. Hensley, and B. D. Tapley (2003), Land subsidence in Houston, Texas, measured by radar interferometry and constrained by extensometers, *J. Geophys. Res.*, *108*(B11), 2542, doi:10.1029/2002JB001848.
Budhu, M. (2008), Mechanisms of earth fissures using the Mohr-Coulomb failure criterion, *Environ. Eng. Geosci.*, *14*(4), 281–295.
Burbey, T., and D. C. Helm (1999), Modeling three-dimensional deformation in response to pumping of unconsolidated aquifers, *Environ. Eng. Geosci.*, *V*(2), 199–212.
Carpenter, M. C. (1993), Earth-fissure movements associated with fluctuations in ground-water levels near the Picacho Mountains, south-central Arizona, 198084, *U.S. Geol. Surv. Prof. Pap.*, 497-H, 49 pp.
Carreón-Freyre, D., M. Cerca, R. Gutierrez-Calderon, and M. H.-L. de Guevara (2010), Monitoring of land subsidence and fracturing in Iztapalapa, Mexico City, in *Land Subsidence, Associated Hazards and the Role of Natural Resources Development, IAHR Publ. 339*, edited by D. Carreón-Freyre et al., pp. 44–50, Int. Assoc. for Hydro-Environ, Wallingford, U. K.
Carreón-Freyre, D., M. Cerca, G. H. Ochoa-González, I. Ortiz-Villaseñor, F. J. Gámez-González, and R. I. Gutiérrez-Calderón (2011), Land subsidence and ground fracturing affecting major cities of central Mexico and related groundwater management, paper presented at the 14th Pan-American Conference on Soil Mechanics and Geotechnical Engineering [CD-ROM], ISSMGE, Toronto, Canada.
Castelletto, N., M. Ferronato, G. Gambolati, M. Putti, and P. Teatini (2008), Can Venice be raised by pumping water underground? A pilot project to help decide, *Water Resour. Res.*, *44*, W01408, doi:10.1029/2007WR006177.
Chaussard, E., S. Wdowinski, E. Cabral-Cano, and F. Amelung (2014), Land subsidence in central Mexico detected by ALOS InSAR time-series, *Remote Sens. Environ.*, *140*, 94–106.
Chen, C. T., J. T. Hu, C. Y. Lu, J. C. Lee, and Y. C. Chan (2007), Thirty-year land elevation change from subsidence to uplift following the termination of groundwater pumping and its geological implications in the Metropolitan Taipei Basin, Northern Taiwan, *Eng. Geol.*, *95*, 30–47.
Chilingarian, G. V., and L. Knight (1960), Relationship between pressure and moisture content of kaolinite, illite, and montmorillonite clays, *AAPG Bull.*, *44*, 101–106.
Colazas, X. C., and R. W. Strehle (1995), Subsidence in the Wilmington oil field, Long Beach, California, USA, in *Subsidence Due to Fluid Withdrawal*, edited by G. V. Chilingarian, E. C. Donaldson, and T. F. Yen, pp. 285–335, Elsevier Sci., Amsterdam, Netherlands.
Collins, P. M. (2007), Geomechanical effects on the SAGD process, *SPE Reservoir Eval. Eng.*, *10*(4), 367–375.
Comerlati, A., M. Ferronato, G. Gambolati, M. Putti, and P. Teatini (2004), Saving Venice by sea water, *J. Geophys. Res.*, *109*, F03006, doi:10.1029/2004JF000119.
Conway, B. D. (2014), Land subsidence monitoring, *Tech. Rep. 2*, 35 pp., Ariz. Dept. of Water Resour, Phoenix, Ariz.
Cooper, H. H., Jr. (1966), The equation of groundwater flow in fixed and deforming coordinates, *J. Geophys. Res.*, *71*(20), 4785–4790.
Corapcioglu, M. Y., and W. Brutsaert (1977), Viscoelastic aquifer model applied to subsidence due to pumping, *Water Resour. Res.*, *13*(3), 597–604.
Dang, V. K., C. Doubre, C. Weber, N. Gourmelen, and F. Masson (2014), Recent land subsidence caused by the rapid urban development in the Hanoi region (Vietnam) using ALOS InSAR data, *Nat. Hazards Earth Syst. Sci.*, *14*, 657–674.
DeWiest, R. J. M. (1966), On the storage coefficient and the equations of groundwater flow, *J. Geophys. Res.*, *71*(4), 1117–1122.
Domenico, P. A., and M. D. Mifflin (1965), Water from low-permeability sediments and land subsidence, *Water Resour. Res.*, *1*(4), 563–576.
Dong, S., S. Samsonov, H. Yin, and S. Ye. (2014), Time-series analysis of subsidence associated with rapid urbanization in Shanghai, China measured with SBAS InSAR method, *Environ. Earth Sci.*, *72*(3), 677–691.
Doornhof, D., T. G. Kristiansen, N. B. Nagel, P. D. Pattillo, and C. Sayers (2006), Compaction and subsidence, *Oilfield Rev.*, *18*(3), 50–68.
Du, J., et al. (2008), Mapping reservoir volume changes during cyclic steam stimulation using tilmeter-based surface deformation measurements, *SPE Reservoir Eval. Eng.*, *11*(1), 63–72.
Ellsworth, W. L. (2013), Injection-induced earthquakes, *Science*, *341*, 142–147.
Erban, L. E., S. M. Gorelick, and H. A. Zebker (2014), Groundwater extraction, land subsidence, and sea-level rise in the Mekong Delta, Vietnam, *Environ. Res. Lett.*, *9*, 084010, doi:10.1088/1748-9326/9/8/084010.
Fallou, S. N., C. C. Mei, and C. K. Lee (1992), Subsidence due to pumping from layered soil: A perturbation technique, *Int. J. Numer. Anal. Methods Geomech.*, *16*, 157–187.
Ferretti, A., C. Prati, and F. Rocca (2001), Permanent scatterers in SAR interferometry, *IEEE Trans. Geosci. Remote Sens.*, *39*(1), 8–20.
Ferretti, A., A. Fumagalli, F. Novali, C. Prati, F. Rocca, and A. Rucci (2011), A new algorithm for processing interferometric data-stacks: SqueeSAR™, *IEEE Trans. Geosci. Remote Sens.*, *49*(9), 3460–3470.
Ferronato, M., G. Gambolati, C. Janna, and P. Teatini (2008), Numerical modelling of regional faults in land subsidence prediction above gas/oil reservoirs, *Int. J. Numer. Anal. Methods Geomech.*, *32*, 633–657.
Ferronato, M., N. Castelletto, G. Gambolati, C. Janna, and P. Teatini (2013), II cycle compressibility from satellite measurements, *Géotechnique*, *63*(6), 479–486.
Feth, J. H. (1951), Structural reconnaissance of the Red Rock Quadrangle, Arizona, *U.S. Geol. Surv. Open File Rep.*, *51–199*, 32 pp.
Figueroa-Vega, G. E. (1984), Case history No. 9.8, Mexico, D.F. Mexico, in *Guidebook to Studies of Land Subsidence Due to Ground-Water Withdrawal*, edited by J. F. Poland, pp. 217–232, UNESCO, Paris.

Finol, A., and Z. A. Sancevic (1995), Subsidence in Venezuela, in *Subsidence Due to Fluid Withdrawal*, edited by G. V. Chilingarian, E. C. Donaldson, and T. F. Yen, pp. 337–372, Elsevier Sci., Amsterdam, Netherlands.
Freeze, R. A. (2000), Social decision making and land subsidence, in *Proceedings of 6th International Symposium on Land Subsidence*, vol. 1, edited by L. Carbognin, G. Gambolati, and A. I. Johnson, pp. 353–384, La Garangola Publ., Padova, Italy.
Frohlich, C. (2012), Two-year survey comparing earthquake activity and injection-well locations in the Barnett Shale, Texas, *Proc. Natl. Acad. Sci. U. S. A.*, *109*, 13,934–13,938.
Fuller, M. (1908), Summary of the controlling factors of Artesian flows, *U.S. Geol. Surv. Bull.*, *319*, 44 pp.
Gabriel, A. K., R. M. Goldstein, and H. A. Zebker (1989), Mapping small elevation changes over large areas: Differential radar interferometry, *J. Geophys. Res.*, *94*(B7), 9183–9191.
Gabrysch, R. K., and R. J. Neighbors (2000), Land-surface subsidence and its control in the Houston-Galveston region, in *Proceedings of 6th International Symposium on Land Subsidence*, edited by L. Carbognin, G. Gambolati, and A. I. Johnson, vol. 2, pp. 91–92, La Garangola Publ., Padova, Italy.
Galloway, D., and F. S. Riley (1999), San Joaquin Valley, California: Largest human alteration of the Earths surface, in *Land Subsidence in the United States, U.S. Geol. Surv. Circ.*, vol. 1182, edited by D. Galloway, D. R. Jones, and S. E. Ingebritsen, pp. 23–34, U.S. Geol. Surv., Denver, Colo.
Galloway, D., D. R. Jones, and S. E. Ingebritsen (Eds.) (1999), Land subsidence in the United States, *U.S. Geol. Surv. Circ.*,1182, 177 pp.
Galloway, D. L., and T. J. Burbey (2011), Review: Regional land subsidence accompanying groundwater extraction, *Hydrogeol. J.*, *19*, 1459–1486.
Galloway, D. L., and J. Hoffmann (2007), The application of satellite differential SAR interferometry-derived ground displacements in hydrogeology, *Hydrogeol. J.*, *15*, 133–154.
Gambolati, G. (1972), A three-dimensional model to compute land subsidence, *Bull. Int. Assoc. Sci. Hydrol.*, *17*(2), 219–226.
Gambolati, G. (1973a), Equation for one dimensional vertical flow of groundwater: 1. The rigorous theory, *Water Resour. Res.*, *9*(4), 1022–1028.
Gambolati, G. (1973b), Equation for one dimensional vertical flow of groundwater: 2. Validity range of the diffusion equation, *Water Resour. Res.*, *9*(5), 1385–1395.
Gambolati, G. (1974), Second order theory of flow in three dimensional deforming media, *Water Resour. Res.*, *10*(6), 1217–1228.
Gambolati, G. (1992), Comment on "Coupling versus uncoupling in soil consolidation" by R. W. Lewis, B. A. Schrefler and L. Simoni, *Int. J. Numer. Anal. Methods Geomech.*, *16*, 833–837.
Gambolati, G., and R. A. Freeze (1973), Mathematical simulation of the subsidence of Venice: 1. Theory, *Water Resour. Res.*, *9*(3), 721–733.
Gambolati, G., and P. Teatini (2014), *Venice Shall Rise Again—Engineered Uplift of Venice Through Seawater Injection, Elsevier Insights* [electronic], 100 pp., Elsevier, Amsterdam, Netherlands.
Gambolati, G., P. Gatto, and R. A. Freeze (1974), Mathematical simulation of the subsidence of Venice: 2. Results, *Water Resour. Res.*, *10*(3), 563–577.
Gambolati, G., P. Gatto, and G. Ricceri (1984), Land subsidence due to gas/oil removal in layered anisotropic soils by a finite element model, in *Proceedings of the Third International Symposium on Land Subsidence*, *IAHS Publ. 151*, edited by A. I. Johnson, L. Carbognin, and L. Ubertini, pp. 29–41, Int. Assoc. of Hydrol. Sci., Wallingford, U. K.
Gambolati, G., G. Ricceri, W. Bertoni, G. Brighenti, and E. Vuillermin (1991), Mathematical simulation of the subsidence of Ravenna, *Water Resour. Res.*, *27*(11), 2899–2918.
Gambolati, G., P. Teatini, L. Tomasi, and M. Gonella (1999), Coastline regression of the Romagna region, Italy, due to sea level rise and natural and anthropogenic land subsidence, *Water Resour. Res.*, *35*(1), 163–184.
Gambolati, G., P. Teatini, D. Baù, and M. Ferronato (2000), The importance of poro-elastic coupling in dynamically active aquifers of the Po river basin, Italy, *Water Resour. Res.*, *36*(9), 2443–2459.
Gambolati, G., M. Ferronato, P. Teatini, R. Deidda, and G. Lecca (2001), Finite element analysis of land subsidence above depleted reservoirs with pore pressure gradient and total stress formulations, *Int. J. Numer. Anal. Methods Geomech.*, *25*(4), 307–327.
Gambolati, G., P. Teatini, and M. Ferronato (2005), Anthropogenic land subsidence, in *Encyclopedia of Hydrological Sciences*, edited by M. G. Anderson, vol. IV, chap. 158, pp. 2444–2459, John Wiley, Chichester, U. K.
Gambolati, G., P. Teatini, M. Ferronato, T. Strozzi, L. Tosi, and M. Putti (2009), On the uniformity of anthropogenic Venice uplift, *Terra Nova*, *21*, 467–473.
Gan, Q., and D. Elsworth (2014), Thermal drawdown and late-stage seismic-slip fault-reactivation in enhanced geothermal reservoirs, *J. Geophys. Res. Solid Earth*, *119*, 8936–8949, doi:10.1002/2014JB011323.
Geerstma, J. (1966), Problems of rock mechanics in petroleum production engineering, in *1st ISRS Congress*, pp. 585–594, Int. Soc. for Rock Mech., Lisbon.
Geerstma, J. (1973), Land subsidence above compacting oil and gas reservoirs, *J. Pet. Technol.*, *25*, 734–744.
Gloe, C. S. (1984), Case history No. 9.1. Latrobe Valley, Victoria, Australia, in *Guidebook to Studies of Land Subsidence Due to Ground-Water Withdrawal*, edited by J. F. Poland, pp. 145–153, UNESCO, Paris.
González, P. J., K. F. Tiampo, M. Palano, F. Cannavó, and J. Fernández (2012), The 2011 Lorca earthquake slip distribution controlled by groundwater crustal unloading, *Nat. Geosci.*, *5*, 821–825.
Häring, M. O., U. Schanz, F. Ladner, and B. C. Dyer (2008), Characterization of the Basel 1 enhanced geothermal system, *Geothermics*, *37*, 469–495.
Helm, D. C. (1975), One-dimensional simulation of aquifer system compaction near Pixley, California: 1. Constant parameters, *Water Resour. Res.*, *11*(3), 465–478.
Helm, D. C. (1976), One-dimensional simulation of aquifer system compaction near Pixley, California: 2. Stress dependent parameters, *Water Resour. Res.*, *12*(3), 375–391.
Helm, D. C. (1984), Field-based computational techniques for predicting subsidence due to fluid withdrawal, in *Man-Induced Land Subsidence, Rev. Eng. Geol.*, vol. VI, edited by T. M. Holzer, pp. 1–22, Geol. Soc. of Am., Boulder, Colo.
Hermann, R. B., and S.-K. Park (1981), The Denver earthquake of 1967–1968, *Bull. Seismol. Soc. Am.*, *71*, 731–745.
Hermansen, H., H. A. Landa, J. E. Sylte, and L. K. Thomas (2000), Experiences after 10 years of waterflooding the Ekofisk Field, Norway, *J. Pet. Sci. Eng.*, *26*, 11–18.
Hernández-Espriú, A., J. A. Reyna-Gutiérrez, E. Sánchez-León, E. Cabral-Cano, J. Carrera-Hernández, P. Martínez-Santos, S. Macías-Medrano, G. Falorni, and D. Colombo (2014), The DRASTIC-Sg model: An extension to the DRASTIC approach for mapping groundwater vulnerability in aquifers subject to differential land subsidence, with application to Mexico City, *Hydrogeol. J.*, *22*(6), 1469–1485.

Hernandez-Marin, M., and T. J. Burbey (2010), Controls on initiation and propagation of pumping-induced earth fissures: Insights from numerical simulations, *Hydrogeol. J.*, *18*(8), 1773–1785.
Hernandez-Marin, M., and T. J. Burbey (2012), Fault-controlled deformation and stress from pumping-induced groundwater flow, *J. Hydrol.*, *428–429*, 80–93.
Higgins, S. A., I. Overeem, A. Tanaka, and J. P. M. Syvitski (2013), Land subsidence at aquaculture facilities in the Yellow River delta, China, *Geophys. Res. Lett.*, *40*, 3898–3902, doi:10.1002/grl.50758.
Higgins, S. A., I. Overeem, M. S. Steckler, J. P. M. Syvitski, L. Seeber, and S. H. Akhter (2014), InSAR measurements of compaction and subsidence in the Ganges-Brahmaputra Delta, Bangladesh, *J. Geophys. Res. Earth Surf.*, *119*, 1768–1781, doi:10.1002/2014JF003117.
Hoffmann, J., H. A. Zebker, D. L. Galloway, and F. Amelung (2001), Seasonal subsidence and rebound in Las Vegas Valley, Nevada, observed by synthetic aperture radar interferometry, *Water Resour. Res.*, *37*(6), 1551–1556.
Hoffmann, J., D. L. Galloway, and H. A. Zebker (2003), Inverse modeling of interbed storage parameters using land subsidence observations, Antelope Valley, California, *Water Resour. Res.*, *37*(2), 1031, doi:10.1029/2001WR001252.
Holland, A. (2013), Earthquakes triggered by hydraulic fracturing in south-central Oklahoma, *Bull. Seismol. Soc. Am.*, *103*, 1784–1792.
Holzer, T. L. (1976), Ground failure in areas of subsidence due to ground-water decline in the United States, in *Proceedings of the II International Symposium on Land Subsidence*, *IAHS Publ. 121*, edited by J. C. Rodda, pp. 423–433, Int. Assoc. of Hydrol. Sci., Wallingford, U. K.
Holzer, T. L. (1981), Preconsolidation stress of aquifer systems in areas of induced land subsidence, *Water Resour. Res.*, *17*(3), 693–704.
Holzer, T. L., and S. N. Davis (1976), Earth fissures associated with water-table declines, *Geol. Soc. Am. Abstr. Programs*, *8*(6), 923–924.
Holzer, T. L., and D. L. Galloway (2005), Impacts of land subsidence caused by withdrawal of underground fluids in the United States, in *Humans as Geologic Agents, Rev. Eng. Geol.*, vol. XVI, edited by J. Ehlen et al., pp. 87–99, Geol. Soc. of Am., Boulder, Colo.
Holzer, T. L., and E. H. Pampeyan (1981), Earth fissures and localized differential subsidence, *Water Resour. Res.*, *17*(1), 223–227.
Holzer, T. L., S. N. Davis, and B. E. Lofgren (1979), Faulting caused by groundwater extraction in southcentral Arizona, *J. Geophys. Res.*, *84*(B2), 603–612.
Horton, S. (2012), Disposal of hydrofracking waste fluid by injection into subsurface aquifers triggers earthquake swarm in central Arkansas with potential for damaging earthquake, *Seismol. Res. Lett.*, *83*, 250–260.
Hsieh, P. (1996), Deformation-induced changes in hydraulic head during groundwater withdrawal, *Ground Water*, *34*(6), 1082–1089.
Huizar-Álvarez, R., L. M. Mitre-Salazar, S. Marín-Córdova, J. Trujillo-Candelaria, and J. Martínez-Reyes (2011), Subsidence in Celaya, Guanajuato, Central Mexico: Implications for groundwater extraction and the neotectonic regime, *Geofis. Int.*, *50*(3), 255–270.
Hung, W.-C., C. Hwang, J.-C. Liou, Y.-S. Lin, and H.-L. Yang (2012), Modeling aquifer-system compaction and predicting land subsidence in central Taiwan, *Eng. Geol.*, *147–148*(6), 78–90.
Hwang, C., W. C. Hung, and C. H. Liu (2008), Results of geodetic and geotechnical monitoring of subsidence for Taiwan high speed rail operation, *Nat. Hazards*, *47*, 1–16.
Ingerson, I. M. (1941), The hydrology of the of the Southern San Joaquin Valley, California, and its relation to important water supplies, *Trans. AGU*, *22*(1), 20–45.
Jachens, R. C., and T. L. Holzer (1979), Geophysical investigations of ground failure related to groundwater withdrawal—Picacho Basin, Arizona, *Ground Water*, *17*(6), 574–585.
Jachens, R. C., and T. L. Holzer (1982), Differential compaction mechanism for earth fissures near Casa Grande, Arizona, *Bull. Geol. Soc. Am.*, *93*(10), 998–1012.
Jacob, C. E. (1940), On the flow of water in elastic artesian aquifer, *Trans. AGU*, *21*(2), 574–586.
Jahr, T., G. Jentzsch, H. Letz, and M. Sauter (2005), Fluid injection and surface deformation at the KTB location: Modelling of expected tilt effects, *Geofluids*, *5*, 20–27.
Janna, C., M. Ferronato, G. Gambolati, and P. Teatini (2010), Simulation of ground failure due to water pumping, in *Land Subsidence, Associated Hazards and the Role of Natural Resources Development, IAHR Publ. 339*, edited by D. Carreón-Freyre et al., pp. 133–135, Int. Assoc. for Hydro-Environ, Wallingford, U. K.
Janna, C., N. Castelletto, M. Ferronato, G. Gambolati, and P. Teatini (2012), A geomechanical transversely isotropic model of the Po River basin using PSInSAR derived horizontal displacement, *Int. J. Rock Mech. Min. Sci.*, *51*, 105–118.
Jha, B., and R. Juanes (2014), Coupled multiphase flow and poromechanics: A computational model of pore pressure effects on fault slip and earthquake triggering, *Water Resour. Res.*, *50*(5), 3776–3808.
Kanamori, H., and D. L. Anderson (1975), Theoretical basis of some empirical relations in seismology, *Bull. Seismol. Soc. Am.*, *65*, 1073–1095.
Kasmarek, M. C., and E. W. Strom (2002), Hydrogeology and simulation of ground-water flow and land-surface subsidence in the Chicot and Evangeline aquifers, Houston area, Texas, *U.S. Geol. Surv. Water Resour. Invest. Rep.*, 024022, 61 pp.
Kim, W.-Y. (2013), Induced seismicity associated with fluid injection into a deep well in Youngstown, Ohio, *J. Geophys. Res. Solid Earth*, *118*, 3506–3518, doi:10.1002/jgrb.50247.
Leake, S. A. (1990), Interbed storage changes and compaction in models of regional groundwater flow, *Water Resour. Res.*, *26*(9), 1939–1950.
Leake, S. A., and D. L. Galloway (2007), MODFLOW ground-water mode: User guide to the subsidence and Aquifer-System Compaction Package (SUB-WT) for water-table aquifers, *U.S. Geol. Surv. Tech. Methods*, Book 6, chap. A23, 42 pp.
Leake, S. A., and D. L. Galloway (2010), Use of the SUB-WT package for MODFLOW to simulate aquifer-system compaction in Antelope Valley, California, USA, in *Land Subsidence, Associated Hazards and the Role of Natural Resources Development, IAHR Publ. 339*, edited by D. Carreón-Freyre et al., pp. 61–67, Int. Assoc. for Hydro-Environ.
Leake, S. A., and D. E. Prudic (1991), Documentation of a computer program to simulate aquifer-system compaction using the modular finite-difference ground-water flow model, *U.S. Geol. Surv. Tech. Water Resour. Invest*, Book 6, chap. A2, 68 pp.
Leonards, G. A. (1962), Engineering properties of soils, in *Foundation Engineering*, edited by G. A. Leonards, pp. 66–240, McGraw-Hill, N. Y.
Lewis, R., and B. Schrefler (1978), A fully coupled consolidation model of the subsidence of Venice, *Water Resour. Res.*, *14*(2), 223–230.
Li, Y., J. Yang, and X. Hu (2000), Origin of ground fissures in the Shanxi Graben System, Northern China, *Eng. Geol.*, *55*, 267–275.
Lofgren, B. E. (1971), Significant role of seepage stresses in compressible aquifer systems, *Eos Trans. AGU*, *52*(11), 832.
Lofgren, B. E., and R. L. Klausing (1969), Land subsidence due to groundwater withdrawal, Tulare-Wasco area, California, *U.S. Geol. Surv. Prof. Pap.*, *437-B*, 101 pp.
Lohaman, S. W. (1961), Compression of elastic artesian aquifers, *U.S. Geol. Surv. Prof. Pap.*, *424-B*, pp. B47–B49.
Mahmoudpour, M., M. Khamehchiyan, M. R. Nikudel, and M. R. Ghassemi (2013), Characterization of regional land subsidence induced by groundwater withdrawals in Tehran, Iran, *Geopersia*, *3*(2), 49–62.
Mazzoldi, A., A. P. Rinaldi, A. Borgia, and J. Rutqvist (2012), Induced seismicity within geological carbon sequestration projects: Maximum earthquake magnitude and leakage potential from undetected faults, *Int. J. Greenhouse Gas Control*, *10*, 434–442.

McCann, G. D., and C. M. Wilts (1951), A mathematical analysis of the subsidence in the Long Beach-San Pedro area, technical report, 119 pp., Calif. Inst. of Technol., Pasadena, Calif.
McNamee, J., and R. E. Gibson (1960), Displacement functions and linear transforms applied to diffusion through porous elastic media, *Q. J. Mech. Appl. Math.*, *13*, 98–111.
Meinzer, O. E. (1928), Compressibility and elasticity of artesian aquifers, *Econ. Geol.*, *23*(3), 263–291.
Meinzer, O. E., and H. A. Hard (1925), The artesian-water supply of the Dakota Sandstone in the North Dakota with special reference to the Edgeley quadrangle, *U.S. Geol. Surv. Water Supply Pap.*, *520-E*, pp. 73–95.
Mitchell, J. K. (1962), Components of pore water pressure and their engineering significance, in *Clays and Minerals*, edited by A. Swineford, pp. 162–184, Pergamon, N. Y.
Motagh, M., T. R. Walter, M. A. Sharifi, E. Fielding, A. Schenk, J. Anderssohn, and J. Zschau (2008), Land subsidence in Iran caused by widespread water reservoir overexploitation, *Geophys. Res. Lett.*, *35*, L16403, doi:10.1029/2008GL033814.
Ng, A. H.-M., L. Ge, X. Li, H. Z. Abidin, H. Andreas, and K. Zhang (2012), Mapping land subsidence in Jakarta, Indonesia using persistent scatterer interferometry (PSI) technique with ALOS PALSAR, *Int. J. Appl. Earth Obs.*, *18*, 232–242.
Ochoa-González, G. H., P. Teatini, D. C. Carréon-Freyre, and G. Gambolati (2013), Modeling the deformation of faulted volcano-sedimentary sequences associated to groundwater withdrawal in the Queretaro Valley, Mexico, in *MODSIM 2013—Adapting to Change: The Multiple Roles of Modelling*, edited by J. Piantadosi et al., pp. 2737–2743, The Model. and Simul. Soc. of Aust. and N. Z. Inc., Canberra, Australia.
Ortega-Guerrero, A., D. L. Rudolph, and J. A. Cherry (1999), Analysis of long-term land subsidence near Mexico City: Field investigations and predictive modelling, *Water Resour. Res.*, *35*(11), 3327–3341.
Ortiz-Zamora, D., and A. Ortega-Guerrero (2010), Evolution of long-term land subsidence near Mexico City: Review, field investigations, and predictive simulations, *Water Resour. Res.*, *46*, W01513, doi:10.1029/2008WR007398.
Pacheco, J., J. Arzate, E. Rojas, M. Arroyo, V. Yutsis, and G. Ochoa (2006), Delimitation of ground failure zones due to land subsidence using gravity data and finite element modeling in the Quertaro valley, Mexico, *Eng. Geol.*, *86*, 143–160.
Phien-wej, N., P. H. Giao, and P. Nutalaya (2006), Land subsidence in Bangkok, Thailand, *Eng. Geol.*, *82*, 187–201.
Pierce, R. L. (1970), Reducing land subsidence in the Wilmington Oil field by use of saline waters, *Water Resour. Res.*, *6*(5), 1505–1514.
Poland, J. F. (1958), Land subsidence due to ground-water development, *J. Irrig. Drain. Div. Am. Soc. Civ. Eng.*, *84*(IR3), 11 pp.
Poland, J. F. (1960), *Land Subsidence in the San Joaquin Valley, California, and Its Effect on Estimates of Ground-Water Resources, Comm. Subterranean Waters Publ. 52*, pp 324–335, Int. Assoc. of Sci. Hydrol.
Poland, J. F. (1961), The coefficient of storage in a region of major subsidence caused by compaction of an aquifer system, *U.S. Geol. Surv. Prof. Pap.*, *424-B*, pp. B52–B54.
Poland, J. F. (Ed.) (1984), *Guidebook to Studies of Land Subsidence Due to Groundwater Withdrawal*, 305 pp., UNESCO, Paris.
Poland, J. F., and G. H. Davis (1956), Subsidence of the land surface in Tulare-Wasco (Delano) and Los Banos-Kettleman City areas, San Joaquin Valley, California, *Trans. AGU*, *37*(3), 287–296.
Poland, J. F., and G. H. Davis (1969), Land subsidence due to withdrawal of fluids, in *Reviews in Engineering Geology*, vol. 2, edited by D. J. Varnes and G. Kiersch, pp. 187–269, Geol. Soc. Am., Boulder, Colo.
Poland, J. F., and J. H. Green (1962), Subsidence in the Santa Clara Valley, California—A progress report, *U.S. Geol. Surv. Water Supply Pap.*, *1619-C*, 16 pp.
Poland, J. F., and B. E. Lofgren (1984), San Joaquin valley, California, U.S.A., in *Guidebook to Studies of Land Subsidence Due to Groundwater Withdrawal*, edited by J. F. Poland, pp. 263–277, UNESCO, Paris.
Poland, J. F., A. A. Garrett, and A. Sinnott (1959), Geology, hydrology, and chemical character of ground waters in the Torrance-Santa Monica area, California, *U.S. Geol. Surv. Water Supply Pap.*, *1461*, pp. 142–146.
Pratt, W. E. (1927), Some questions on the cause of the subsidence of the surface in the Goose Creek field, Texas, *Am. Assoc. Pet. Geol. Bull.*, *11*(8), 887–889.
Pratt, W. E., and D. W. Johnson (1926), Local subsidence of the Goose Creek oil field, *J. Geol.*, *XXXIV*(7), Part 1, 577–590.
Qu, F., Q. Zhang, Z. Lu, C. Zhao, C. Yang, and J. Zhang (2014), Land subsidence and ground fissures in Xian, China 2005–2012 revealed by multi-band InSAR time-series analysis, *Remote Sens. Environ.*, *155*, 366–376, doi:10.1016/j.rse.2014.09.008.
Rappleye, H. S. (1933), Recent areal subsidence found in releveling, *Eng. News Rec.*, *110*, p. 848.
Raspini, F., C. Loupasakis, D. Rozos, and S. Moretti (2013), Advanced interpretation of land subsidence by validating multi-interferometric SAR data: The case study of the Anthemountas basin (Northern Greece), *Nat. Hazards Earth Syst. Sci.*, *13*, 2425–2440.
Riley, F. S. (1986), Developments in borehole extensometry, in *Proceedings of the 3rd International Symposium on Land Subsidence*, *IAHS Publ. 151*, edited by A. I. Johnson et al., pp. 169–186, Int. Assoc. of Hydrol. Sci., Wallingford, U. K.
Rintoul, W. (1981), The case of disappearing land, in *Drilling Ahead: Tapping California's Richest Oil Field*, pp. 116–137, Valley Publ., Santa Cruz, Calif.
Rivera, A., E. Ledoux, and G. de Marsily (1991), Nonlinear modeling of groundwater flow and total subsidence of the Mexico City aquifer-aquitard system, in *Proceedings of 4th International Symposium on Land Subsidence*, *IAHS Publ. 200*, edited by A. I. Johnson, pp. 44–58, Int. Assoc. of Hydrol. Sci., Wallingford, U. K.
Russell, W. L. (1928), The origin of artesian pressure, *Econ. Geol.*, *23*(2), 132–157.
Safai, N. M., and G. Pinder (1979), Vertical and horizontal land deformation in a desaturating porous medium, *Adv. Water Resour.*, *2*, 19–25.
Safai, N. M., and G. Pinder (1980), Vertical and horizontal land deformation due to fluid withdrawal, *Int. J. Numer. Anal. Methods Geomech.*, *4*, 131–142.
Schiffman, R. L., A. T. F. Chen, and J. C. Jordan (1969), An analysis of consolidation theories, *J. Soil Mech. Found. Div. Am. Soc. Civ. Eng.*, *65*(SM1), 285–312.
Schmidt, D. A., and R. Burgmann (2003), Time dependent land uplift and subsidence in the Santa Clara Valley, California, from a large InSAR data set, *J. Geophys. Res.*, *108*(B9), 2416, doi:10.1029/2002JB002267.
Shau, P., and P. K. Sikdar (2011), Threat of land subsidence in and around Kolkata City and East Kolkata Wetlands, West Bengal, India, *J. Earth Syst. Sci.*, *120*(3), 435–446.
Sheng, Z., and D. C. Helm (1998), Multiple steps of earth fissuring caused by ground-water withdrawal, in *Current Research and Case Studies: Proceedings of the Joseph F. Poland Symposium on Land Subsidence*, edited by J. Borchers, pp. 229–238, Star Publ. Co., Belmont, Calif.
Sheng, Z., D. C. Helm, and J. Li (2003), Mechanisms of earth fissuring caused by groundwater withdrawal, *Environ. Eng. Geosci.*, *9*(4), 313–324.
Shi, X., Y. Xue, S. Ye, J. Wu, Y. Zhang, and J. Yu (2007), Characterization of land subsidence induced by groundwater withdrawals in Su-Xi-Chang area, China, *Environ. Geol.*, *52*(1), 27–40.

Snider, L. C. (1927), A suggested explanation of the surface subsidence in the Goose Creek oil and gas field, Texas, *Am. Assoc. Pet. Geol.*, *11*(7), 729–745.
Sreng, S. L., H. Sugiyama, T. Kusaka, and M. Saitoh (2011), Upheaval phenomenon in clay ground induced by rising groundwater level, in *Poromechanics IV*, edited by H. I. Ling et al., pp. 196–203, DEStech Publ., Lancaster, Pa.
Stancliffe, R. P. W., and M. W. A. van der Kooij (2001), The use of satellite-based radar interferometry to monitor production activity at the Cold Lake heavy oil field, Alberta, Canada, *AAPG Bull.*, *85*(5), 781–793.
Strozzi, T., U. Wegmüller, L. Tosi, G. Bitelli, and V. Spreckeks (2001), Land subsidence monitoring with differential SAR interferometry, *Photogramm. Eng. Remote Sens.*, *67*(11), 1261–1270.
Taylor, D. W. (1948), *Fundamentals of Soil Mechanics*, 700 pp., John Wiley, N. Y.
Teatini, P., G. Gambolati, and L. Tosi (1995), A new 3-D non-linear model of the subsidence of Venice, in *Proceedings of 5th International Symposium on Land Subsidence*, IASH Publ. 234, edited by F. B. J. Barends et al., pp. 353–361, Int. Assoc. of Hydrol. Sci., Wallingford, U. K.
Teatini, P., M. Ferronato, G. Gambolati, and M. Gonella (2006), Groundwater pumping and land subsidence in the Emilia-Romagna coastland, Italy: Modeling the past occurrence and the future trend, *Water Resour. Res.*, *42*, W01406, doi:10.1029/2005WR004242.
Teatini, P., M. Ferronato, G. Gambolati, D. Ba, and M. Putti (2010), Anthropogenic Venice uplift by seawater pumping into a heterogeneous aquifer, *Water Resour. Res.*, *46*, W11547, doi:10.1029/2010WR009161.
Teatini, P., N. Castelletto, M. Ferronato, G. Gambolati, and L. Tosi (2011a), A new hydrogeological model to predict anthropogenic Venice uplift, *Water Resour. Res.*, *47*, W12507, doi:10.1029/2011WR010900.
Teatini, P., G. Gambolati, M. Ferronato, T. Settari, and D. Walters (2011b), Land uplift due to fluid injection, *J. Geodyn.*, *51*, 1–16.
Teatini, P., et al. (2011c), Geomechanical response to seasonal gas storage in depleted reservoirs: A case study in the Po River basin, Italy, *J. Geophys. Res. - Earth Surf.*, *116*, F02002, doi:10.1029/2010JF001793.
Teatini, P., L. Tosi, and T. Strozzi (2012), Comment on "Recent subsidence of the Venice Lagoon from continuous GPS and interferometric synthetic aperture radar" by Y. Bock, S. Wdowinski, A. Ferretti, F. Novali, and A. Fumagalli, *Geochem. Geophys. Geosyst.*, *13*, Q07008, doi:10.1029/2012GC004191.
Teatini, P., N. Castelletto, and G. Gambolati (2014), 3D geomechanical modelling for CO_2 geological storage: A case study in an offshore northern Adriatic reservoir, Italy, *Int. J. Greenhouse Gas Control*, *22*, 63–76.
Terzaghi, K. (1923), Die berechnung des durchlassigkeitsziffer des tones aus dem verlauf der hydrodynamischen spannungserscheinungen, *Sitzungsber. Akad. Wiss. Wien Math. Naturwiss. Kl.*, *132*, Abt. 2A, 125–138.
Terzaghi, K., and R. B. Peck (1948), *Soil Mechanics in Engineering Practice*, 566 pp., John Wiley, N. Y.
The Royal Society and the Royal Academy of Engineering (2012), *Shale Gas Extraction in the UK: A Review of Hydraulic Fracturing*, London, U. K. [Available at https://royalsociety.org/policy/projects/shale-gas-extraction/2012-06-28-shale-gas.pdf.]
Theis, C. V. (1935), The relationship between the lowering of the piezometric surface and the rate and duration of discharge of a well using groundwater storage, *Trans. AGU*, *16*, 519–524.
Thu, T. M., and D. G. Fredlund (2000), Modelling subsidence in the Hanoi City area, Vietnam, *Can. Geotech. J.*, *37*, 621–637.
Todd, D. K. (1960), *Groundwater Hydrology*, 2nd ed., 552 pp., John Wiley, N. Y.
USEPA (2002), Technical program overview: Underground control regulations, *Tech. Rep. EPA 816-R-02-025*, 81 pp., Washington, D. C.
Vasco, D. W., A. Rucci, A. Ferretti, A. Novali, R. C. Bissell, P. S. Ringrose, A. S. Mathieson, and I. W. Right (2010), Satellite-based measurements of surface deformation reveal flow associated with the geological storage of carbon dioxide, *Geophys. Res. Lett.*, *37*, L03303, doi:10.1029/2009GL041544.
Verruijt, A. (1969), Elastic storage of aquifers, in *Flow Through Porous Media*, edited by R. De Wiest, pp. 331–376, Academic, New York.
Verruijt, A. (1995), *Computational Geomechanics*, 387 pp., Kluwer Acad. Publ., Dordrecht, Netherlands.
Wang, G. Y., G. You, and B. Shi (2009), Earth fissures triggered by groundwater withdrawal and coupled by geological structures in Jiangsu Province, China, *Environ. Geol.*, *57*(5), 1047–1054.
Wegmüller, U., C. Werner, T. Strozzi, and A. Wiesmann (2004), Multitemporal interferometric point target analysis, in *Analysis of Multi-Temporal Remote Sensing Images, Ser. Remote Sens.*, vol. 3, edited by P. Smits and L. Bruzzone, pp. 136–144, World Sci., Hoboken, N. J.
Wilson, A. M., and S. Gorelick (1996), The effects of pulsed pumping on land subsidence in the Santa Clara Valley, California, *J. Hydrol.*, *174*, 375–396.
Wolf, R. G. (1970), Relationship between horizontal strain near a well and reverse water level fluctuation, *Water Resour. Res.*, *6*(6), 1721–1728.
Wu, J., X. Shi, S. Ye, Y. Xue, Y. Zhang, Z. Wei, and Z. Fang (2010), Numerical simulation of viscoelastoplastic land subsidence due to groundwater overdrafting in Shanghai, China, *J. Hydrol. Eng.*, *15*(3), 223–236.
Ye, S., Y. Xue, J. Wu, and Q. Li (2012), Modeling visco-elastic-plastic deformation of soil with modified Merchant model, *Environ. Earth Sci.*, *66*(5), 1497–1504.
Yeh, A., and M. J. O. Sullivan (2007), Modelling land subsidence in geothermal fields, in *Proceedings of 29th New Zealand Geothermal Workshop* [CD-ROM], 9 pp., Univ. of Auckland, Auckland, New Zealand.
Yu, J., Z. Li, and J. Wu (2009), Land subsidence in the Changzhou-Wuxi region mapped by InSAR/GPS integration approach, *Prog. Nat. Sci.*, *19*(11), 1267–1271.
Yu, J., G. Wang, T. J. Kearns, and L. Yang (2014), Is there deep-seated subsidence in the Houston-Galveston area? *Int. J. Geophys.*, *2014*, 11, doi:10.1155/2014/942834.
Xue, Y., Y. Zhang, S. Ye, J. Wu, and Q. Li (2005), Land subsidence in China, *Environ. Geol.*, *48*(6), 713–720.
Zaman, M. M., A. Abdulraheem, and J. C. Roegiers (1995), Reservoir compaction and surface subsidence in the north sea Ekofisk field, in *Subsidence Due to Fluid Withdrawal*, edited by G. V. Chilingarian et al., pp. 373–423, Elsevier Sci., Amsterdam, Netherlands.
Zanello, F., P. Teatini, M. Putti, and G. Gambolati (2011), Long term peatland subsidence: Experimental study and modeling scenarios in the Venice coastland, *J. Geophys. Res.*, *116*, F04002, doi:10.1029/2011JF002010.
Zhang, Y., H. Gong, Z. Gu, R. Wang, X. Li, and W. Zhao (2014), Characterization of land subsidence induced by groundwater withdrawals in the plain of Beijing city, China, *Hydrogeol. J.*, *22*(2), 397–409.
Zhao, C., X. Ding, Q. Zhang, Z. Lu, and Z. Li (2008), Monitoring of recent land subsidence and ground fissures in Xian with SAR interferometry, *Int. Arch. Photogramm. Remote Sens. Spatial Inf. Sci.*, *XXXVII*(Part B1), 147–150.
Zhu, L., H. Gong, P. Teatini, B. Chen, and R. Wang (2015), Land subsidence due to the groundwater over-exploration in the northern Beijing plain, *China, Env. Geol.*, doi:10.1016/j.enggeo.2015.04.020.
Ziaie, A., K. Kumarci, A. R. Ghanizadeh, and A. Mahmodinejad (2009), Prediction of earth fissures development in Sirjan, *Res. J. Environ. Sci.*, *3*(4), 486–496.
Zimmerman, R. (1991), *Compressibility of Sandstones, Developments in Petroleum Science*, vol. 29, 183 pp., Elsevier, Amsterdam, Netherlands.
Zoback, M. D. (2007), *Reservoir Geomechanics*, 452 pp., Cambridge Univ. Press, Cambridge, U. K.